Chapter 6
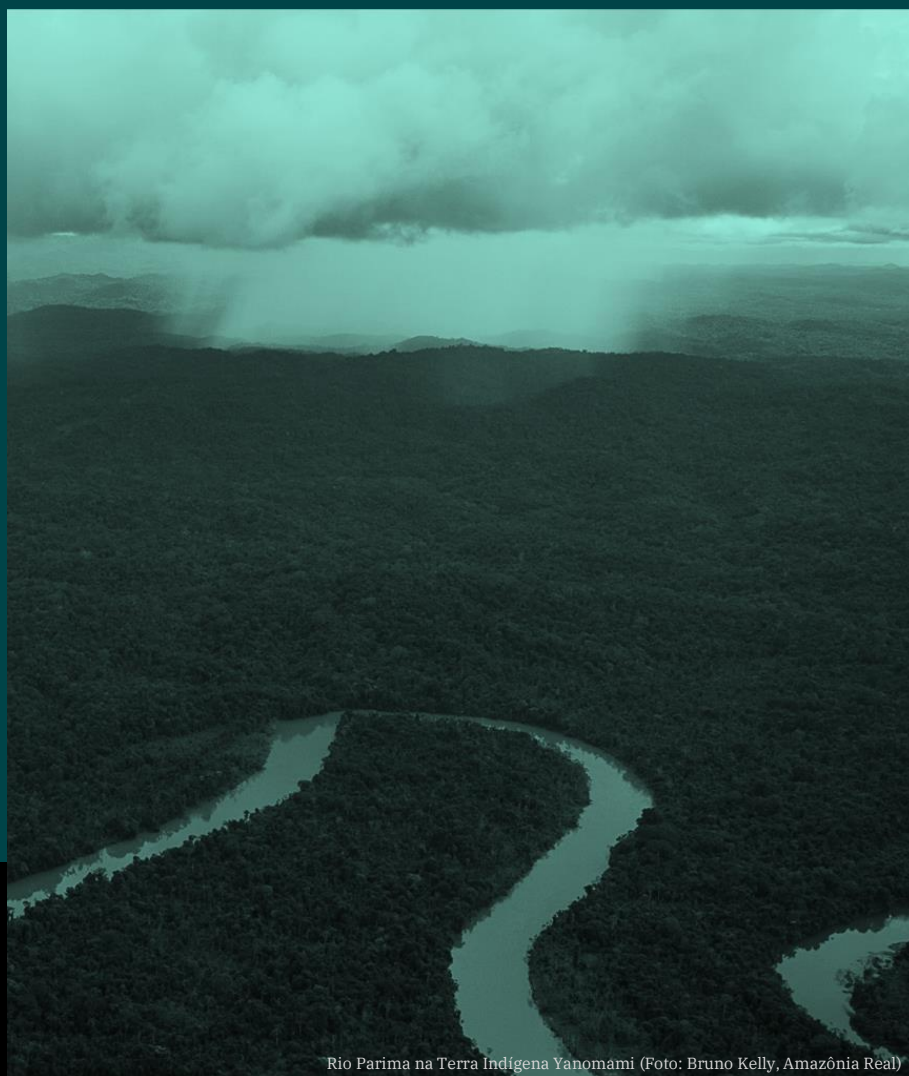
Biogeochemical cycles in the Amazon

Rio Parima na Terra Indígena Yanomami (Foto: Bruno Kelly, Amazônia Real)

THE AMAZON WE WANT

Science Panel for the Amazon

SUSTAINABLE DEVELOPMENT SOLUTIONS NETWORK
A GLOBAL INITIATIVE FOR THE UNITED NATIONS

About the Science Panel for the Amazon (SPA)

The Science Panel for the Amazon is an unprecedented initiative convened under the auspices of the United Nations Sustainable Development Solutions Network (SDSN). The SPA is composed of over 200 preeminent scientists and researchers from the eight Amazonian countries, French Guiana, and global partners. These experts came together to debate, analyze, and assemble the accumulated knowledge of the scientific community, Indigenous peoples, and other stakeholders that live and work in the Amazon.

The Panel is inspired by the Leticia Pact for the Amazon. This is a first-of-its-kind Report which provides a comprehensive, objective, open, transparent, systematic, and rigorous scientific assessment of the state of the Amazon's ecosystems, current trends, and their implications for the long-term well-being of the region, as well as opportunities and policy relevant options for conservation and sustainable development.

INDEX

Graphical Abstract

Amazon ecosystems represent a large component of the global carbon cycle, accounting for ~16% of terrestrial productivity, representing uptake by photosynthesis of about 20 billion tons of carbon per year.

Biogenic volatiles as well as primary and secondary organic aerosols affect cloud condensation processes and rainfall.

An intact Amazonian ecosystem stores large amounts of carbon above and below ground, totaling about 200 billion tonnes of carbon.

Forest disturbances can lead to an increase of atmospheric CO_2, while the intact Amazon forests are a carbon sink that helps to reduce the rate of global warming.

Amazon basin is estimated to represent 6-8% of global methane emissions. Aquatic environments in the Amazon release considerable amounts of methane while uptake and release of CO_2 are approximately in balance.

River

Shallow Water

Low Várzea | High Várzea

High productivity of the Amazon forest is facilitated by efficient recycling of phosphorus and nitrogen compounds by soil organisms and vegetation.
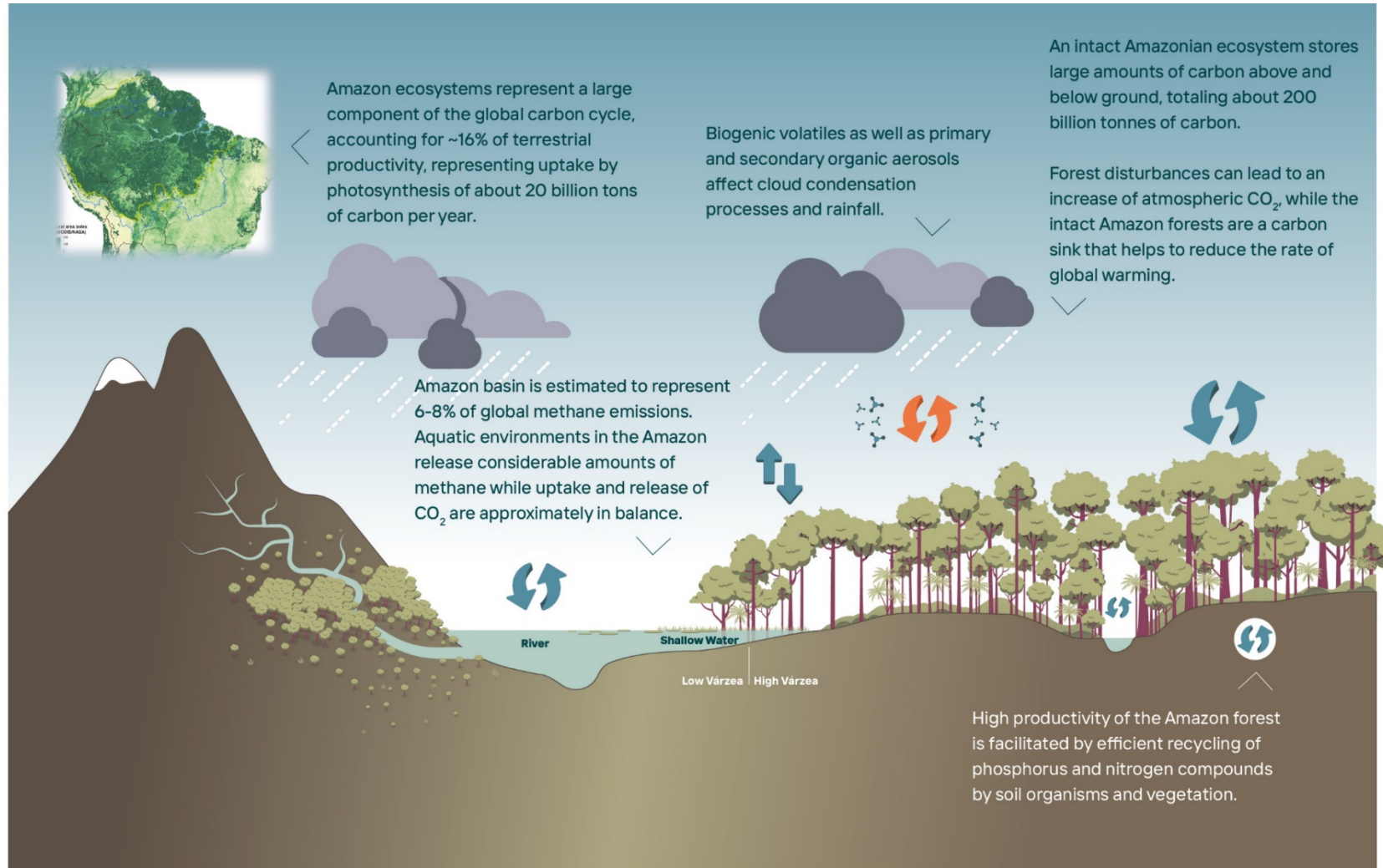
Figure 6.A Graphical Abstract.

Biogeochemical Cycles of the Amazon

Yadvinder Malhi*ᵃ, John Melack*ᵇ, Luciana V. Gattiᶜᵈ, Jean Omettoᵇ, Jürgen Kesselmeierᵉ, Stefan Wolff ᵉ, Luiz E.O. Aragãoᵇᶠ, Marcos Costaᵍ, Scott Saleskaʰ, Sunitha R. Pangalaⁱ, Luana S. Bassoᵇ, Luciana Rizzoʲ, Alessandro C. de Araùjoʲ, Natalia Restrepo-Coupeᵏ, Celso H.L. Silva Juniorᶜˡ

Key Messages

- The Amazon forest is a major store and ongoing sink of carbon that makes a modest contribution to reducing carbon dioxide levels in the atmosphere. This carbon sink has been weakening over recent decades.
- Available estimates of carbon inputs from plants growing in seasonally inundated habitats are of similar order to estimates of CO_2 degassed from these habitats. Hence, aquatic environments would seem to be approximately in balance, though inputs from uplands do add some inorganic and organic carbon.
- Methane emissions from the Amazon Basin are estimated to represent 6-8% of global methane emissions, though large uncertainties in both sources and sinks remain.
- The Amazon region contributes a large fraction of global N_2O emissions from natural ecosystems; biological N fixation is a major source of available nitrogen for the regional biosphere.
- The release of biogenic volatiles from the forest plays an important role in cloud condensation, affecting rainfall.

Abstract

The Amazon basin hosts the Earth's largest extent of tropical forest and the world's largest river system. These two features make it a major contributor to regional and global biogeochemical cycles, such as the carbon cycle and major nutrient cycles. This chapter summarizes our understanding of the cycles of three key biogeochemical elements in the Amazon (carbon, nitrogen, and phosphorus), spanning both terrestrial and aquatic ecosystems. Historically, the intact Amazon biome has been a major carbon sink, though this sink appears to be weakening over time. The chapter also examines the net emissions of two other key trace gases with substantial contributions to radiative warming (methane and dinitrogen oxide), and trace gas and aerosol emissions and their impact on atmospheric pollution, cloud properties, and water cycling.

Keywords: carbon, carbon dioxide, methane, nitrogen, phosphorus, aerosols, clouds, aquatic, terrestrial

[a] Environmental Change Institute, School of Geography and the Environment, University of Oxford, South Parks Road, Oxford OX1 3QY, UK, yadvinder.malhi@ouce.ox.ac.uk

[b] Bren School of Environmental Science and Management, University of California, Bren Hall 2400, Santa Barbara CA 93117, USA

[c] Nuclear and Energy Research Institute, IPEN-CNEN/SP, Av. Prof. Lineu Prestes, 2242, Butantã, São Paulo SP 05508-000, Brazil

[d] Earth System Science Center (CCST), National Institute for Space Research (INPE), Av. dos Astronautas, 1.758, Jardim da Granja, São José dos Campos SP 12227-010, Brazil

[e] Multiphase Chemistry Department, Max Planck Institute for Chemistry, Hahn-Meitner-Weg 1, 55128 Mainz, Germany

[f] College of Life and Environmental Sciences, University of Exeter, Stocker Road, Exeter EX4 4PY, UK

[g] Department of Agricultural Engineering, Federal University of Viçosa, Av. Peter Henry Rolfs, Viçosa MG 36570-900, Brazil

[h] Department of Ecology and Evolutionary Biology, University of Arizona, Tucson AZ 85721, USA

[i] Lancaster Environment Centre, Lancaster University, Library Avenue, Bailrigg, Lancaster LA1 4YQ, UK

[j] Empresa Brasileira de Pesquisa Agropecuária (EMBRAPA), Travessa Dr Eneas Pinheiro, Belèm PA, Brazil

[k] School of Life Sciences, University of Technology Sydney, 15 Broadway, Ultimo NSW 2007, Australia

[l] Universidade Estadual do Maranhão (UEMA), Cidade Universitária Paulo VI, Avenida Lourenço Vieira da Silva, 1000, Jardim São Cristovão, 65055-310 São Luís, MA, Brazil

6.1 Introduction

The Amazon basin accounts for around 16% of the entire metabolism of the terrestrial biosphere and is the largest drainage basin in the world, contributing around one-fifth of global freshwater discharge. These features make it a major contributor to regional and global biogeochemical cycles, including the cycles of carbon, nitrogen, phosphorus, and other nutrients. This chapter highlights and summarizes some of the main aspects of the biogeochemistry of the Amazon region. The focus is to understand baseline or natural biogeochemical processes in relatively intact regions of the Amazon. Deforested and other human-modified landscapes are discussed in Part II of this report. However, where we draw up budgets for the whole region (of carbon or methane), we include anthropogenic emissions in order to have a complete picture. This chapter starts with first considering the carbon cycle of Amazon, its seasonal variability, and the role of the intact Amazon forest as a carbon sink. Subsequent sections describe the cycling of key nutrients in the Amazon (nitrogen and phosphorus). Then we consider the region's contribution to global budgets of other major greenhouse gases, methane and N_2O. Finally, we turn to emissions of other biogenic trace gases and aerosols, and their role in affecting cloud physics and dynamics and ozone chemistry.

When considering the literature on the biogeochemical cycles of the Amazon region as a whole, it is important to define what is meant by the Amazon. Different studies use different definitions. For example, forest carbon cycle studies tend to focus on the whole lowland forest biome, including areas outside of the Amazon watershed (e.g., the Guyanas) but exclude non-lowland forest biomes such as the planalto and the Andean montane regions. In contrast, hydrological studies tend to focus on the entire watershed. Here, we adopt the definitions of Eva *et al.* (2005). The five regions of Amazon *sensu lato* (the whole Amazon-Tocantins watershed plus adjoining lowland forest regions) are the Amazon Basin lowland forests (5,569,174 km²),

Guyana lowland forests (970,161 km²), Gurupi lowland forests (161,463 km²), the non-forest biome Amazon watershed in the planalto (864,951 km²) and the montane Andes in the Amazon watershed (555,564 km²). The narrowest definition (lowland forest biome within the Amazon Basin) is also referred to as the Amazon *sensu stricto*. Please refer to the Annex on geographic limits and meanings for further exploration of this issue.

We first focus on forest biomass carbon dynamics; the Amazon holds a great deal of carbon in aboveground biomass; therefore, the forest and its fate are linked to the global carbon cycle. However, water availability and nutrients can limit productivity and affect carbon cycling; we discuss the water, nitrogen, and phosphorus cycles. We then focus attention on two other important greenhouse gases with significant sources in the Amazon: methane and nitrous oxide. Finally, forests are linked to climate not only through their ability to evaporate water, but through the production of gases and aerosols that in turn influence radiation, cloud properties, and precipitation. Our focus throughout is on largely intact ecosystems in Amazon, mainly forests and freshwaters, but under recent and current climate and atmospheric conditions. Hence, these intact ecosystems are not equivalent to pre-industrial Amazonian ecosystems. Degraded and extensively modified Amazonian ecosystems are discussed in Part II of this report.

6.2 Carbon Cycle in the Amazon

6.2.1 The Amazon carbon cycle throughout the Cenozoic and Pleistocene

The South American broadleaf tropical forest biome probably began to take its modern, closed-canopy, angiosperm-dominated structure in the wake of the Chicxulub asteroid impact 66 million years ago, and the associated extinction of megafaunal dinosaurs (Carvalho *et al.* 2021) (see Chapter 1). In the warm, humid climates of the Paleogene (66-23 Ma), "tropical" (or megathermal, i.e. not affected by frost) forests covered much of South

America, connecting the proto-Amazon and Atlantic Forest biomes and extending much further south to Patagonia (Maslin *et al.* 2005). The suitable climate and high atmospheric CO_2 concentrations of this early "mega-Amazon" could have resulted in substantially higher productivity and overall biomass than the modern Neotropical biome. Over the last 50 million years, CO_2 concentrations have broadly declined, and there has been an associated cooling and drying of the global and regional climate. Tropical forests have retreated, the Atlantic Forest separated from the Amazonian biome (Maslin *et al.* 2005), and grasses spread from Africa in the Late Miocene (~10 Ma), resulting in the creation of new, fire-dominated savanna biomes such as the cerrado, and the further retreat of the forest (Osborne *et al.* 2007). Carbon stocks and ecosystem productivity are likely to have declined along with these atmospheric changes.

Over the Pleistocene (2.6 Ma - 11.7 Ka), the establishment of large, northern ice caps greatly amplified climate instability. These ice caps enabled ice-albedo feedbacks. Slight cooling (warming) led to further expansion (retreat) of ice sheets, leading to increased (decreased) reflection of solar radiation, and by extension amplification of small changes in Earth's rotation and orbit into dramatic changes in climate. The last 1 million years have been dominated by a roughly 100,000-year cycle, 90% of which is largely a cool climate with low atmospheric CO_2 (~180 ppm) and high climate variability, broken by short (~10,000-year periods) of warmer and wetter conditions, higher CO_2 (~280 pm), and less climate variability (the Holocene being a prime example). Low CO_2 concentrations of glacial periods (180 ppm) may be close to the threshold of viability of photosynthesis and would have reduced ecosystem productivity.

There has been much speculation as to how Amazonian forests varied during these glacial-interglacial cycles. Haffer (1969) famously suggested that during glacial maxima the forest biome retreated into refugia separated by cerrado, and this process was a driver of Amazonian speciation. This sce-

nario has not stood the test of time; the broad consensus seems to be that during glacial periods there was only modest retreat in forest extent at the boundaries. Paleoecological and speleotherm data suggest that the climate was undoubtedly drier, but the lower temperatures reduced evapotranspiration rates and enabled forest to persist (Mayle *et al.* 2004, Bush *et al.* 2017, Wang *et al.* 2017). However, substantial areas of forest may have been dry forests interweaved between moist rainforests. The variability of the climate may have enabled an occasional corridor of savanna to open in the eastern Amazon. Overall, Amazonian carbon stocks are likely to have been only slightly reduced from present-day values, but productivity would have been substantially reduced and the rate of carbon cycling slower (Mayle *et al.* 2004).

In the latest interglacial period, the Holocene (11.7 Ka – present), rainforest productivity and carbon stocks initially increased with warmer, wetter, and higher CO_2 conditions. However, over the early- to mid-Holocene (ca. 8,500–3,600 yr BP), reduced precipitation and increased fire frequency affected much of the south of the region, resulting in forest retreat and expansion of savanna and dry forest (Mayle *et al.* 2004). In the Late Holocene, the rain belt expanded further south, and the forest gradually expanded southwards, resulting in an overall increase in the Amazon's forest biomass to peak values in the last thousand years (Mayle *et al.* 2004).

6.2.2 Carbon cycle processes in terrestrial Amazonian forests

6.2.2.1 Amazon Forest Carbon Cycle

The Amazon forest biome stores around 90 Pg C in above- and below-ground vegetation biomass (Saatchi *et al.* 2007). Soil carbon stocks are of similar magnitude to vegetation biomass carbon (Malhi *et al.* 2009, de Oliveira Marques *et al.* 2017), and hence total carbon stocks of the Amazon forest biome are ~150-200 Pg C. Some of the soil carbon is in non-labile fractions relatively resistant to forest cover loss, but a large part is in labile forms near
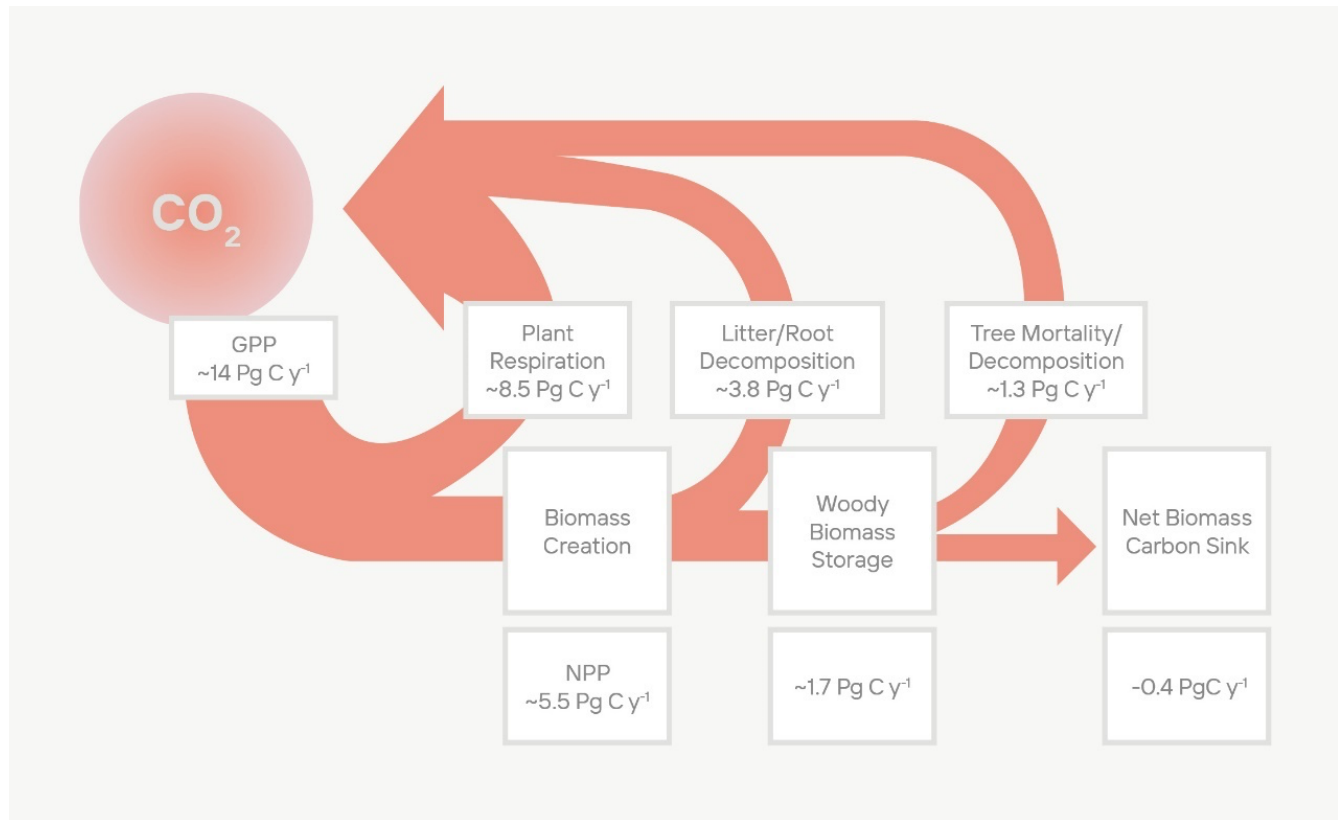
Figure 6.1 Some of the key concepts in the terrestrial carbon cycle (the numbers indicated are for the entire Amazon forest biome). Plants take up carbon dioxide through photosynthesis: this is the Gross Primary Productivity (GPP). Much of the carbon is used for plant metabolism and respiration, with the remainder being used to produce biomass including wood, leaves and fine roots. The short-lived tissue is rapidly shed and decomposed, releasing carbon dioxide back to the atmosphere as heterotrophic respiration. Carbon in woody tissue and soils tends to accumulate over time through ecological succession but is mostly released back to the atmosphere through tree mortality and decomposition. Overall, the processes of woody biomass creation and tree mortality have not been in balance in recent decades, leading to a net biomass carbon sink, equivalent to positive Net Biome Productivity (NBP). Data are extrapolated to the area of the Amazon forest biome using values provided in Malhi *et al.* (2016) and Brienen *et al.* (2015).

the surface that are vulnerable to loss (de Oliveira Marques *et al.* 2017).

The net carbon balance of terrestrial Amazonian systems is the resultant of large fluxes of uptake and release. With their year-long growing season, tropical forests such as those in the Amazon are amongst the most productive natural ecosystems on Earth. A range of studies across the basin describe the carbon cycle processes of Amazonian forests. Figure 6.2 illustrates the carbon cycle of a typical central Amazonian forest near Manaus, Brazil, derived from (Malhi *et al.* 2009).

Input of carbon to the forest through photosynthesis is termed gross primary productivity (GPP); typically, about one-third of GPP is used for biomass production of wood, fine roots, leaves, and reproductive tissues (net primary productivity or fine root tissues are short-lived and make up a small proportion of total biomass stocks. All biomass ends up as dead material, either through litterfall, herbivory, or mortality. This material is broken down and metabolized, primarily by fungi but also by bacteria and soil macrofauna such as termites, releasing carbon dioxide to the atmosphere as heterotrophic respiration. There are additional, sma-
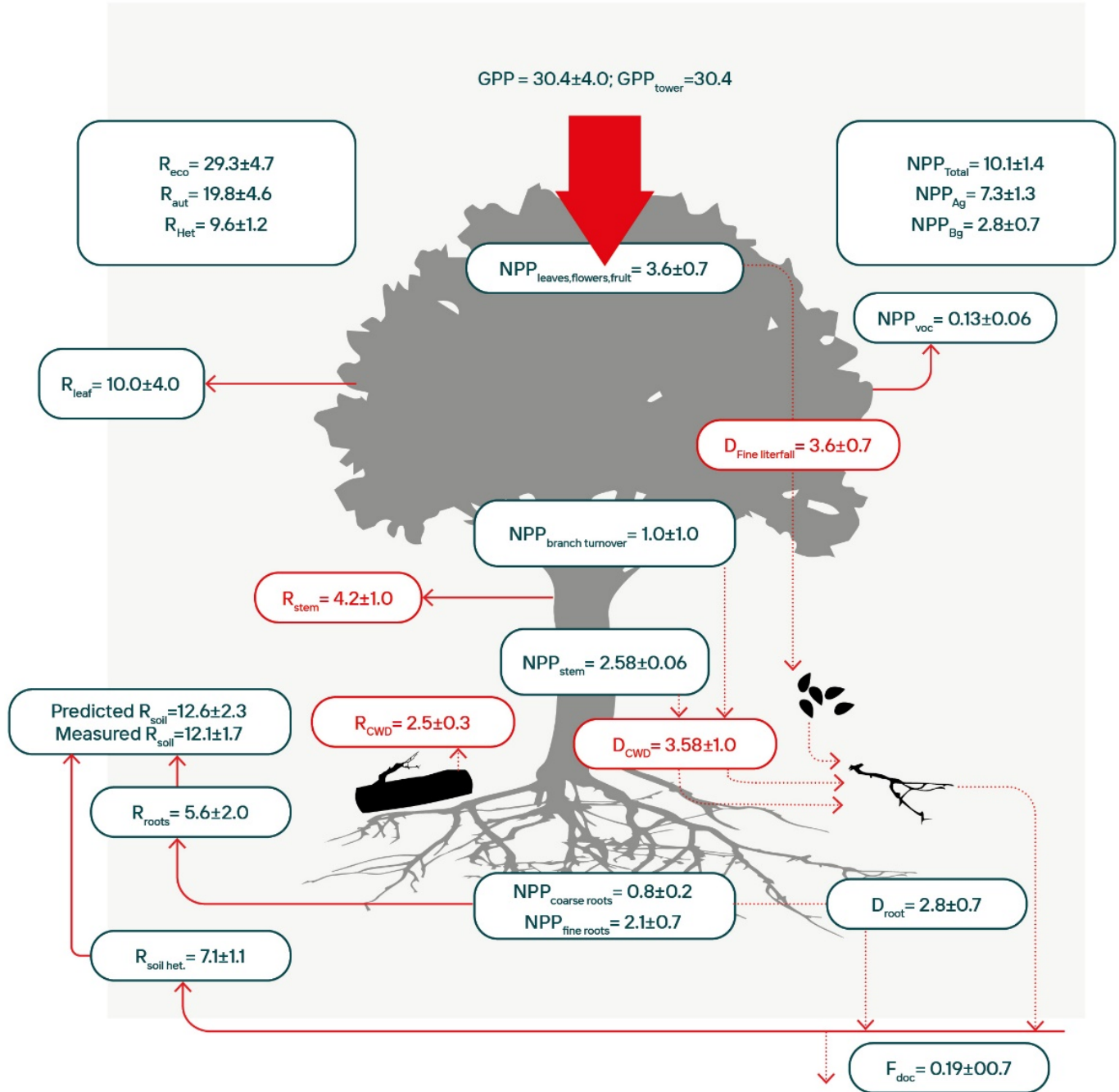
Figure 6.2. The carbon cycle of a typical Amazonian forest (near Manaus, central Amazon). Adapted from data in Malhi et al. (2009a). GPP = Gross Primary Productivity (predicted as sum of NPP and autotrophic respiration, and directly estimated from flux tower measurements (NEE + Reco); NEE - net carbon flux or net ecosystem exchange, Reco - combination of autotrophic and heterotrophic respiration, NPP - Net Primary Productivity, in total, and above ground (AG) and belowground (BG) components, and its components as (i) canopy production (leaves, flower, fruit, twigs); (ii) branch turnover; (iii) volatile organic carbon emissions (VOC); (iv) above-ground woody tissue production (stem); (v) coarse root production; (vi) fine root production; R - Respiration, in total and autotrophic (aut) and heterotrophic (het) components, and its components as (vii) leaf respiration; (viii) wood tissue respiration; (ix) root respiration; (x) soil heterotrophic respiration; (xi) total soil respiration, either directly measured or predicted as sum of inputs assuming no net change in soil carbon stocks; D - detritus fluxes, as (xii) fine litterfall; (xiii) coarse woody debris production; (xiv) root detritus production; (xv) Fdoc - carbon export in the form of dissolved organic carbon. Units are Mg C ha^{-1} y^{1}.

ller fluxes to and from the ecosystem; volatile organic compounds, such as isoprenoids (isoprene, monoterpenes, sequiterpenes), and methane account for more than 0.5% of GPP (Kesselmeier *et al.* 2002), and outflow of dissolved organic carbon in stream water is less than 1% of GPP, though this fraction will vary by soil and vegetation and is not well sampled. The net carbon balance of a mature *terra firme* Amazonian forest could be expected to be zero from ecological first principles, as the uptake of carbon through photosynthesis is compensated by releases of carbon through heterotrophic and autotrophic respiration. However, long term inventories suggest a net rate of increase of vegetation biomass of 0.6 Mg C ha^{-1} y^{-1} (where Mg is 10^6 grams) (see below), equivalent to about 2% of photosynthesis (Brienen *et al.* 2015).

6.2.2.2 Variation of GPP and NPP Across the Amazon and Their Relation to Climate, Geology, and Hydrology

The total GPP of the Amazon is around 20 Pg C y^{-1}, accounting for around 16% of global terrestrial GPP (Beer *et al.* 2010). There are relatively few direct measurements of NPP and GPP across the Amazon. Broadly, the magnitude of GPP is determined more by seasonality in rainfall rather than soil nutrient status, with the highest values found in the wet forests of the northwestern Amazon, and lower values in regions with a long dry season, where photosynthesis rates in the dry season are reduced by either stomatal closure or by increasing deciduousness (Malhi *et al.* 2015). The highest productivities reported for the Amazon are in the aseasonal and relatively fertile forests near Iquitos in Peru (Malhi *et al.* 2015). Sandy soils, such as those found in the upper Rio Negro Basin, support lower productivity. However, rates of NPP and woody biomass production do not follow the same regional pattern, and higher rates of woody growth tend to be found in the western Amazon. This may be because the soils of the western Amazon tend to have higher nutrient content (Malhi *et al.* 2004), reflecting their younger age, geological history, and soil structure (Quesada *et al.* 2012). There is a strong gradient in tree turnover across the Amazon, with trees in the western and southern Ama-

zon tending to both grow faster and die younger, and trees in the eastern Amazon (and especially the Guyana shield) being slow-growing and long-lived (Quesada *et al.* 2012). This change in dynamics affects the patterns of biomass, with the highest biomass (and vegetative carbon stock) in Amazonian forests tending to be found in the northeastern Amazon (Johnson *et al.* 2016). Hence, in mature forests, rates of tree growth are negatively correlated with forest biomass, and tree mortality and turnover rates influence biomass more strongly than productivity and tree growth rates. In montane systems in the Andes, the productivity of forests declines with elevation, halving by about 3,000 m elevation (Malhi *et al.* 2018). Forest turnover rates show no trend with elevation, so forest biomass declines in proportion to declining productivity.

Both the magnitude and nature of soil carbon stocks are highly variable across the Amazon. Soil types range from highly-weathered ferralsols which dominate the eastern parts of the Basin, through to a predominance of younger soils in the western basin and lower montane slopes, occasional patches of sandy soils, and carbon-rich organic soils dominating in wetland regions, such as northern Peru, and montane cloud forests (Quesada *et al.* 2020).

6.2.2.3 Seasonal Variation of the Carbon Cycle

Plant phenology — the timing of cyclic or recurrent biological events, such as leaf, stem, or root growth; leaf senescence; or flowering — is a sensitive indicator of plant and forest function that links seasonal climate rhythms to the seasonality of carbon cycle processes (Albert *et al.* 2019, Reich *et al.* 2004, Jones *et al.* 2014, Saleska *et al.* 2003). The seasonality of GPP fluxes emerges from the phenology of leaf growth and senescence (Wu *et al.* 2016, Lopes *et al.* 2016, Wagner *et al.* 2017), while that of soil respiration is likely linked to climate seasonality and the phenology of both leaves and fine root dynamics (Keller *et al.* 2004, Raich 2017, Girardin *et al.* 2016). Seasonality of soil respiration is also buffered by deep soil CO_2 production, which lags

surface soil CO_2 production due to slower drying of deep soil horizons in the dry season (Davidson *et al.* 2004). Understanding how seasonal rhythms of biology, climate, and resources interact to regulate carbon fluxes is thus a key part of understanding and predicting forest drought response, resilience, and future change.

GPP seasonality exhibits distinct patterns across the Amazon; including a notable contrast readily seen from space, ground surveys, or eddy flux towers; between dry season increases in GPP ("greening") in intact rainforest regions of the central Amazon versus seasonal declines ("browning") in converted forests, southern forests, or savanna woodlands (Figure 6.3). There is debate over these patterns and the mechanisms driving them (including whether they might be remote sensing artefacts (Huete *et al.* 2006, Morton *et al.* 2014, Saleska *et al.* 2016), and how they might be modeled (Lee *et al.* 2005, Baker *et al.* 2008, Restrepo-Coupe *et al.* 2017), but recent work combining flux data, satellites, phenocams, and leaf-level data suggests they emerge from patterns of water availability (Guan *et al.* 2015) and root distribution (Ivanov *et al.* 2012; Brum *et al.* 2019), sunlight (Restrepo-Coupe *et al.* 2013), and plant phenological strategy (Wu *et al.* 2016, Wagner *et al.* 2017).

Seasonal variation in biosphere functioning couple carbon and water exchanges with the atmosphere and contribute to global scale seasonal variations in atmospheric CO_2 and H_2O. Because leaf stomata link evapotranspiration to GPP, dry season maxima in GPP facilitate a corresponding dry season maxima in forest ET (Shuttleworth 1988, Hasler and Avissar 2007; see Chapter 7). By moistening the dry season atmospheric boundary layer, these fluxes hasten the transition to the wet season ahead of the southward migration of the intertropical convergence zone (Wright *et al.* 2017, Fu and Li 2004).

6.2.2.4 The net carbon sink in intact Amazonian forests

Old-growth forests are, in principle, in long-term equilibrium, with woody biomass growth balanced by mortality, and photosynthesis equal to the sum of autotrophic and heterotrophic respiration plus a minor amount exported to streams and rivers (Figure 6.2), with a net carbon balance of zero. In practice, an old-growth forest stand may not be carbon neutral because of (i) long term episodic disturbance and recovery; (ii) large, long-lived trees that may continue to accumulate biomass for many centuries or even millennia; (iii) secular atmospheric changes, such as rising CO_2 concentration, or changes in temperature or rainfall may lead to long-term trends in productivity and/or respiration. The RAINFOR network has monitored aboveground biomass changes in Amazon, and currently spans over 400 plots across the region. The network's observations suggest an increase in biomass in old growth forests over time, summing to 0.38 (0.28-0.49 95% C.I.) Pg C year^{-1} if extrapolated over the Amazon forest biome in the 2000s (Brienen *et al.* 2015) (Figure 6.4). This accumulation seems to stop in drought years (Phillips *et al.* 2009) and seems to be declining over time (Brienen *et al.* 2015). Increasing length of the dry season may lead to the intact forests of the Amazon becoming a carbon source in the near future (see Chapter 19). The widespread nature of the observed biomass accumulation (plus similar observations from Africa and Borneo) suggests that a global driver such as increasing atmospheric CO_2 could be responsible for this net carbon sink (Hubau *et al.* 2020, Qie *et al.* 2019). An alternative possibility is recovery from past anthropogenic disturbance (with accessible sites more likely to have been disturbed in the past), although the timescales involved (>100 years) and the observation of increasing growth rates over time argue against this possibility.

6.2.2.5 The Amazon's contribution to atmospheric oxygen

Terrestrial carbon fluxes are mirrored by oxygen fluxes; photosynthesis absorbs carbon from the atmosphere and releases an equivalent number of molecules of oxygen, and respiration releases carbon dioxide and consumes oxygen. As intact Amazonian forests are currently a net carbon sink, as described above, they must be a net oxygen source.
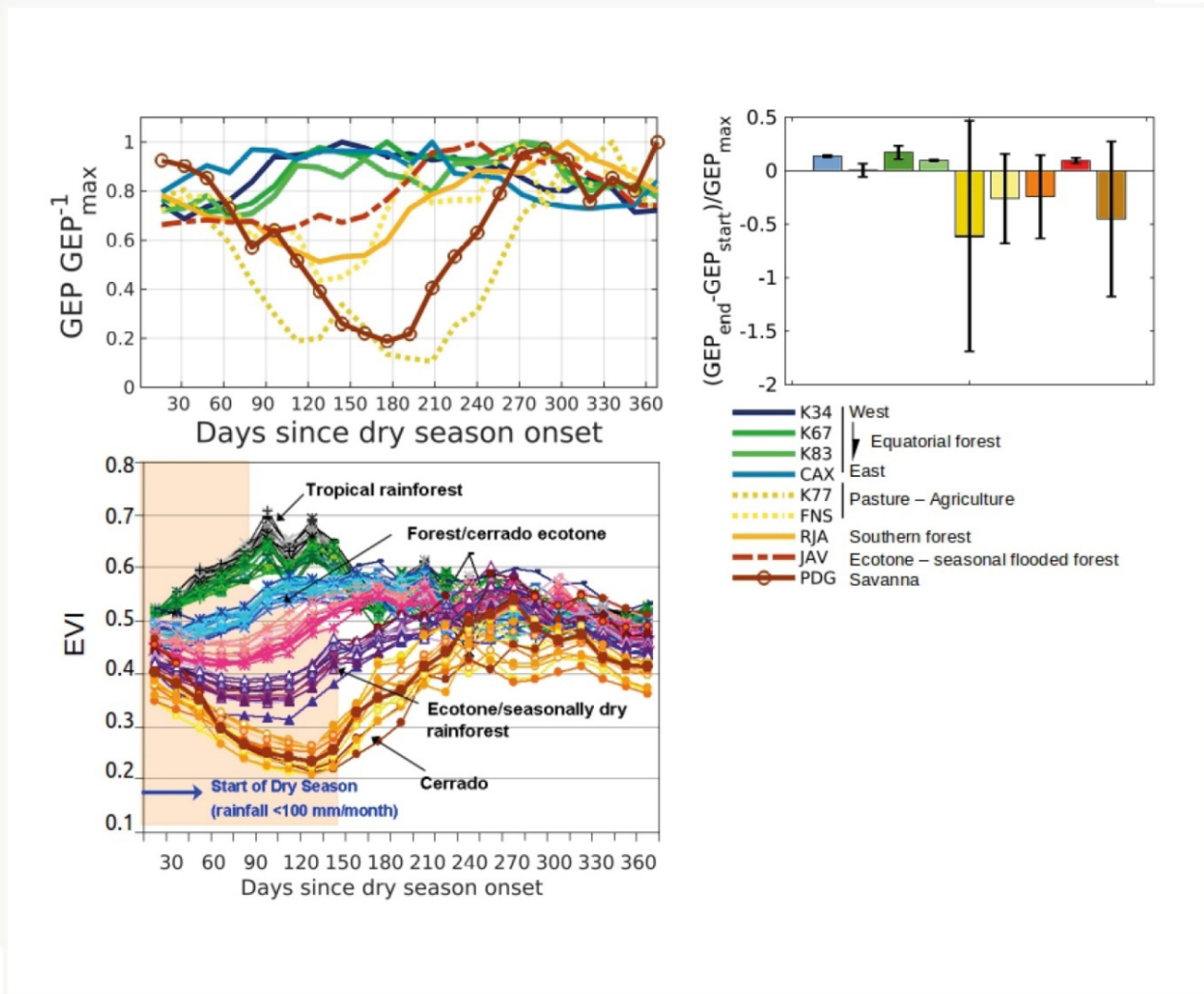
Figure 6.3 (upper left panel) Dry season gross primary productivity (GPP), photosynthetic flux, relative to maximum at each site (GPP GPP$_{max}^{-1}$) dynamics versus number of days since dry-season onset, across different sites in Amazon (see legend to the right, with equatorial forests in green/blue solid lines, southern forest orange line, pastures as dotted yellow lines, ecotone forest as dashed, and cerrado in solid brown). (upper right panel) GPP fractional change during the dry season, relative to its magnitude at start of the dry season (error bars indicate site-specific interannual variability) (modified from Restrepo-Coupe *et al.* (2013)). (lower panel) MODIS enhanced vegetation index (EVI) across an ecotone from Santarém forests to cerrado near Cuiabá (modified from Ratana *et al.* 2012, 2006).

This has led to the widespread perception that the Amazon is essential to the oxygen supply, and that losing the Amazon forest would lead to a significant decrease in oxygen. This perception is incorrect. The crucial difference between carbon dioxide and oxygen is that the current atmospheric stock of CO_2 is ~415 ppm, whereas the current atmospheric oxygen stock is ~21%, or 21,000 ppm.

Hence a rate of increase of CO_2 of 2 ppm per decade (the approximate contribution of tropical deforestation) is significant (~0.5% per decade), but the corresponding decrease of oxygen (~0.002% per decade) is negligible. On the timescale of thousands of years the Amazon is likely in approximate net carbon and oxygen balance, with photosynthesis balanced by respiration; large stocks of atmos-

pheric oxygen were instead built up over millions of years mainly by ocean phytoplankton. There are many reasons for concern for the Amazon, but loss of oxygen is not one of them.

6.2.3 Disturbances as Modifiers of the Amazonian Carbon Cycle

The steady state of the Amazonian carbon cycle can be disrupted abruptly, with long-lasting effects, by forest disturbances, both natural and anthropogenic. These can be associated with climate-driven intensification of seasonal cycles (Barichivich *et al.* 2018, Gouveia *et al.* 2019), which can be exacerbated by the interaction between deforesta-
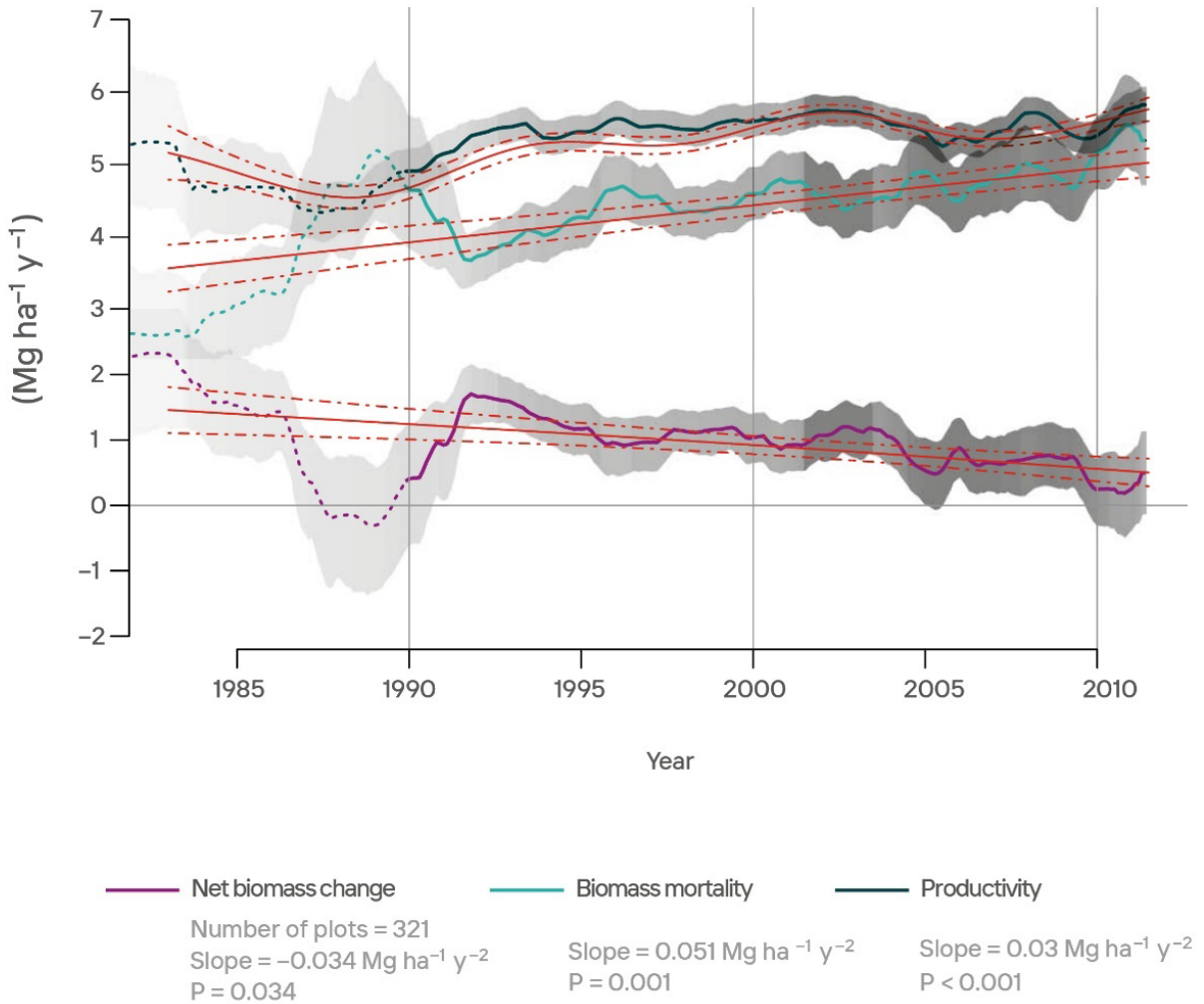
Figure 6.4. Long-term carbon dynamics of structurally intact old growth tropical forests in Amazon (adapted from Brienen *et al.* 2015) Trends in net aboveground live biomass carbon (a), carbon gains to the system from wood production (b), and carbon losses from the system from tree mortality (c), measured in 321 forest inventory plots. Black lines show the overall mean change up to 2011 for 321 plots (or 274 units) weighted by plot size, and its bootstrapped confidence interval (shaded area). The red lines indicate the best model fit for the long-term trends since 1983 using general additive mixed models (GAMM), accounting explicitly for differences in dynamics between plots (red lines denote overall mean, broken lines denote standard error of the mean).

tion and climate change (Zemp *et al.* 2017), increasing the frequency of flooding, windstorms, and droughts. On the other hand, changes in the frequency and intensity of extreme climatic events, especially droughts, can favor human-induced forest disturbances related to human-ignited fires, which can lead to forest degradation. The combination of climatic and anthropogenic processes tend to reinforce each other (Cochrane 2001; Cochrane & Laurance 2002, 2008; Alencar, Solorzano & Nepstad 2004; Aragão *et al.* 2007, 2008; Poulter *et al.* 2010, Zemp *et al.* 2017), exacerbating any single forcing impact.

6.2.3.1 Direct Climate Effect on the Carbon Cycle

Blowdowns are meteorological processes caused by downbursts associated with convective squall lines, resulting in large patches of tree mortality by uprooting or breaking tree trunks (Espirito-Santo *et al.* 2014, Araujo *et al.* 2017). These events can cause significant gross losses of carbon from aboveground live biomass, with large (≥5 ha, blowdowns only) and intermediate (0.1–5 ha, blowdowns plus other causes of death) events contributing to ~0.3% (~0.003 Pg C y^{-1}), and ~1.1% (~0.01 Pg C y^{-1}) of the loss. Most of the natural gross C loss, however, is concentrated in small (<0.1 ha) canopy disturbances accounting for ~98.6% (~1.28 Pg C y^{-1}) of total forest-dynamics related losses over the entire Amazon region (Figure 6.1; Espirito-Santo *et al.* 2014, where Pg is 10^{15} g). Despite the magnitude of impacts on C stocks, recovery of disturbed patches promotes net biomass accumulation that approximately balances observed losses. Forests disturbed by blowdowns tend, however, to be more susceptible to the effects of other forest disturbances, such as droughts and fires. The impact of droughts may be larger in these forests due to changes in plant community composition and structure, favoring early successional species with fast growth rates (Nelson *et al.* 1994), which are characterized by low wood density and susceptibility to drought (Phillips *et al.* 2009, 2010). The accumulation of dead wood from tree mortality can further destabilize the C cycle by increasing

forest vulnerability to fire, if these areas are near human-ignition sources.

The frequency of interannual climate variations (e.g., recurring droughts or periods of excess wetness due to El Niño and the Southern Oscillation (ENSO) cycles, and associated occurrence of fires or blowdowns) structure Amazonian forests' functional composition and carbon cycling. Forest carbon cycle responses to interannual droughts and temperature variations in different biogeographic regions provide insights into forest function, resilience, and carbon cycling.

Drought-induced stress from water limitation in *terra firme* forests can reduce the overall capacity of the forest system to uptake atmospheric CO_2 and increase tree mortality in old growth Amazonian forests (Phillips *et al.* 2010, van der Molen *et al.* 2011) (see Section 23.1.3 in Chapter 23). Drought can directly reduce the photosynthetic capacity of forests by promoting stomatal closure (Santos *et al.* 2018, Smith *et al.* 2020, Garcia *et al.* 2021) and/or inducing leaf shedding (Doughty *et al.* 2015, Anderson *et al.* 2010), and can contribute to excess mortality. Tree vulnerability to drought, however, varies across the functional diversity of tree species, with species having more resilient hydraulic architecture (e.g., greater embolism resistance of their water-transporting xylem) less likely to succumb to drought (Rowland *et al.* 2015). This is consistent with developing ecohydrological theories of tree response to drought (Anderegg *et al.* 2018, Wu *et al.* 2020, Wang *et al.* 2020) that suggests forest vulnerability to drought is heterogeneous across the Amazon, depending on forest species composition, functional traits, and local environments (Cosme *et al.* 2017, Oliveira *et al.* 2019, Esquivel-Muelbert *et al.* 2020, Barros *et al.* 2019, Aleixo *et al.* 2019, Castro *et al.* 2020).

Declines in photosynthetic uptake and/or increases in mortality are responsible for a reduction in aboveground (Nepstad *et al.* 2004, Phillips *et al.* 2009, da Costa *et al.* 2010) and belowground biomass production (Metcalfe *et al.* 2008). In addition

to the reduction in carbon assimilation by vegetation, increased tree mortality has an additive effect on the reduced capacity of Amazonian forests to assimilate and store atmospheric carbon. Droughts tend to weaken or even reverse the net Amazonian forest sink (Gatti *et al.* 2014). The net carbon sink is quantified as net biome productivity (NBP; Figure 6.1) and its reduction is the result of the additive effect of declines in photosynthesis during drought and subsequent increases in heterotrophic respiration in the following wet season (Tian *et al.* 1998, Zeng *et al.* 2008), driven by widespread drought-induced tree mortality increasing the decomposing pool (Williamson *et al.* 2000, Phillips *et al.* 2009). Droughts, such as that of 2005, can, therefore, promote biomass loss from tree mortality (approximately -1.1 [95% C.I. -2.04 to -0.49] Pg C), with an additional NPP reduction of -0.50 Pg C (Phillips *et al.* 2009). Assuming an exponential wood decomposition rate of 0.17 y^{-1} (Chambers *et al.* 2000), it is expected that annual emissions from this pool of dead wood one year after a drought account for -0.18 (95% CI from -0.32 to -0.07) Pg C, steadily reducing over time (Aragão *et al.* 2014). While it did not experience excessive drought in 2005, the central Amazon also lost biomass carbon due to blowdowns associated with a single synoptic storm event (Chambers *et al.* 2014); thus, some biomass losses attributable to climate variability can be through processes other than mortality directly related to drought stress.

Hydrologic environments significantly structure drought response; seasonally inundated floodplain forests, in contrast to *terra firme* forests discussed above, are limited by hypoxia (low oxygen) and thus droughts, rather than increasing forest stress, relieve it and induce increases in growth and NPP (Schöngart and Wittmann 2011). However, these areas are vulnerable to altered hydroperiods, as indicated by increased mortality in floodplains influenced by dams that modulate discharge and inundation (Resende *et al.* 2020). Recent studies show that even in *terra firme* forests, shallow water table regions with greater access to soil water show neutral or positive responses to drought, with decreased mortality and increases in recruitment

and growth (Sousa *et al.* 2020, Esteban *et al.* 2020). Accounting for the difference between deep water table forests with limited water access, deep water table forests with large soil water storage capacity (Nepstad *et al.* 1994, Oliveira *et al.* 2005, Guan *et al.* 2015), and shallow water table forests with greater water access (one third of Amazonian *terra firme* forests) appears to reconcile earlier controversies over differences between remote sensing (which showed vegetation green up [Saleska *et al.* 2007, Brando *et al.* 2010, Samanta *et al.* 2010, Janssen *et al.* 2021]) and plot scale studies in deep water table regions (which showed negative responses to drought). An important research priority is to improve understanding of the influence of both environmental and organismal functional heterogeneities to arrive at a more integrated understanding of forest responses to environmental perturbations such as drought (Longo *et al.* 2018, Levine *et al.* 2016).

6.2.3.2 Human-Induced Fire Disturbances

Natural fires in the Amazon are rare (see Chapter 5). Human-induced land use and cover change is a major factor determining fire occurrence in Amazonian forests as they are directly related to ignition sources. Human activities associated with droughts can exacerbate the occurrence of fires in the Amazon and induce their spread into adjacent forest areas, altering the carbon cycle. Old-growth forests exposed to droughts (associated with low rainfall, increases in temperature, vapor pressure deficit (VPD) inside the canopy (Ray *et al.* 2005), decreases in relative humidity (Cardoso *et al.* 2003, Sismanoglu and Setzer 2005), and decreases in plant available water (PAW) (Nepstad *et al.* 2004) are more prone to the incursion of fires related to deforestation or agricultural land management. One of the most uncertain components of Amazonian forest fire impacts is the magnitude of short- and long-term carbon emissions, potential implications for CO_2 levels in the atmosphere, and consequent global warming. Quantification of carbon emissions from understory forest fires is still lacking, preventing accurate estimates of the contribution of this component. Van der Werf *et al.* (2010)
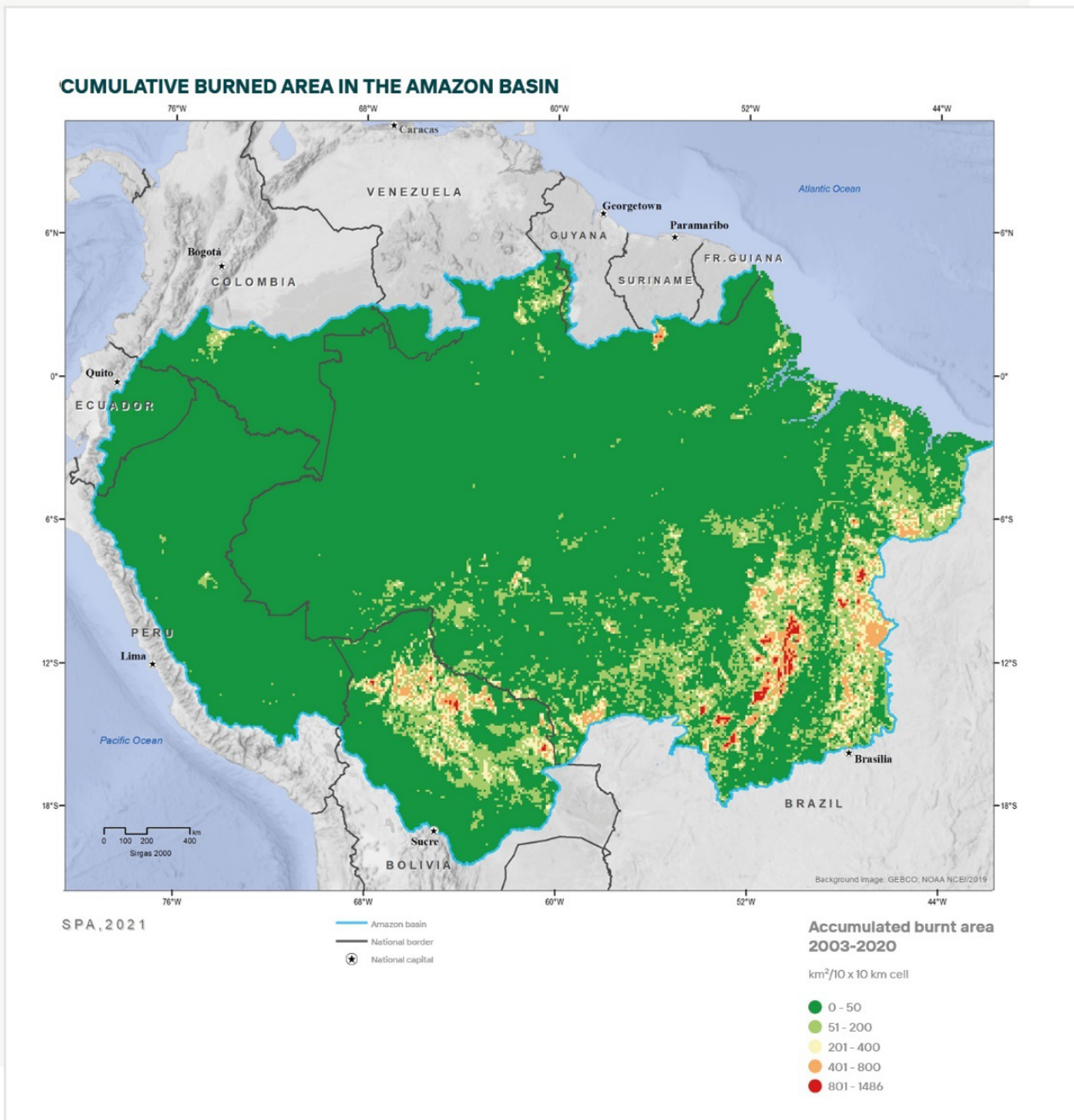
Figure 6.5. Spatial distribution of the cumulative burned area in the Amazon basin from 2003 to 2020 based on the MODIS MCD64A1 C6 product.

estimated for the period between 1997 to 2009 that globally fires were responsible for an annual mean carbon emission of 2.0 Pg C y^{-1}, with South America contributing 14.5%. Of this, about 8% appears to have been associated with forest fires, based on estimates from the Global Fire Emission Dataset (GFED) for South America. According to Silva *et al.* (2020), forest fires contribute cumulative gross emissions of carbon of ~126 Mg CO_2 ha^{-1} for 30 years after a fire event and a mean annual efflux of 4.2 Mg CO_2 ha^{-1} y^{-1}. This same study showed that cumulative CO_2 uptake of burned forests offsets only 35% (45.0 Mg CO_2 ha^{-1}) of the total gross emissions from forest fires within the same timeframe. Emissions from the decomposition of the dead organic matter account for ca. 58% (47.4 Mg CO_2 ha^{-1}) of total net emissions (Silva *et al.* 2020). The total contribution to the basin will depend on the burned area which can vary widely between drought and non-drought years. In the Brazilian Amazon between 2008 and 2012 an average of 7,800 km^2 of old-growth forest were affected by fires, with a peak of 25,400 km^2 during the 2010 drought (Aragão *et al.* 2018). For the whole Amazon, data from MODIS MCD64A1 C6 (Figure 6.5) demonstrate that an area of about 151,412±62,253 km^2 (mean±sd) km^2 $year^{-1}$ has burned in the last 18 years. It also suggests that, within this period, c.a. 60,000 km^2 of burned area occurred in areas already deforested and in areas mapped as primary forests in the year 2000 (Aragão *et al.* 2014). Forest fires result from the leakage of fires from deforested areas to adjacent forests (Aragão *et al.* 2016). Apart from at the driest fringes, most of the Amazon region is not naturally fire susceptible and its ecosystems are not resilient to fires.

6.2.4 Carbon Cycle Processes in Aquatic Amazonian Ecosystems

The uptake, release, and transport of carbon by aquatic Amazonian ecosystems is a significant component of the regional carbon cycle. High rates of primary production by plants and algae in aquatic environments, considerable sedimentation in lakes and reservoirs, and large amounts of carbon dioxide and methane emitted from rivers, lakes, and wetlands all lead to fluxes disproportionately large relative to the area of aquatic systems (Melack *et al.* 2009, Melack 2016). Remote sensing analyses of inundation and wetland habitats, inundation modeling, and extensive and intensive measurements in rivers, reservoirs, lakes, and wetlands are now available, but considerable uncertainty and information gaps remain given the diverse aquatic habitats throughout the Amazon Basin. Aquatic habitats range from headwater streams to lakes and floodplains fringing rivers. Junk *et al.* (2011) delineated major types of wetlands in the lowland Amazon based on climate, hydrology, water chemistry, and botany. Hess *et al.* (2015) used synthetic aperture radar (SAR) data at 100 m resolution to determine inundated area and areal extent of major aquatic habitats (open water, herbaceous plants, and flooded forests) within the lowland basin (<500 m). The amplitude, duration, and frequency of inundation determine the temporal and spatial variations of these aquatic habitats and associated fluxes. Multi-year time series of inundation at 0.25° resolution, and recently at 0.5 to 1 km resolution, derived from several satellite-borne sensors, are available (Hamilton *et al.* 2002, Prigent *et al.* 2020, Parrens *et al.* 2019). Hydrological models (e.g., Coe *et al.* 2007, Paiva *et al.* 2013) calculate river discharges well, while a paucity of digital elevation models on floodplains compromises inundation estimates.

Exchange of carbon dioxide and methane between surface water and the overlying atmosphere depends on the concentration gradient between air and water and on physical processes at the interface, usually parameterized as gas transfer velocity (k). Methane can also exit via bubbles and pass through the tissues of rooted aquatic plants, both herbaceous and woody. Water to atmosphere fluxes of carbon dioxide from all aquatic environments in the catchments of the Amazon and Tocantins river systems, covering approximately 970,500 km^2, are estimated to be approximately 722 Tg C y^{-1} (where Tg is 10^{12} grams) (Table 6.1).

Fluxes from hydroelectric reservoirs add 8.85 Tg C y^{-1}. Of the total, excluding hydroelectric reservoirs, fluxes from river channels represent about 19%, streams about 14%, floodable forests 36%, and

other wetlands plus a small contribution from the open water of lakes and reservoirs about 30%. While terrestrial sources of dissolved organic carbon (DOC) and particulate organic carbon (POC) contribute to these fluxes, the majority of the carbon released to the atmosphere is likely derived from organic matter in aquatic plants photosynthesizing with atmospheric CO_2 (Melack and Engle 2009). Hence, most of these water-to-atmosphere fluxes represent respiration of carbon fixed within aquatic habitats, not carbon transported from uplands. To estimate net fluxes from aquatic habitats, a portion of the aquatic NPP must be subtracted from the total fluxes listed in Table 6.1.

Floodplains and other wetlands are productive aquatic environments that export considerable amounts of carbon to rivers, accumulate sediments, and provide a portion of the organic carbon that leads to the evasion of CO_2 and CH_4 to the atmosphere. Melack *et al.* (2009) summarized estimates of net primary productivity (NPP) for the plants and algae on central Amazon floodplains. The total net production attributed to flooded forests (excluding wood increments), aquatic macrophytes, phytoplankton, and periphyton within the 1.77 million km^2 portion of the Basin characterized by Hess *et al.* (2003) is about 300 Tg C y^{-1}. Flooded forests account for 62% of the total, aquatic macrophytes 34%, and the remaining 4% is associated with periphyton and phytoplankton.

Approximately 10% of the total value equals the export of organic carbon by the Amazon River (Richey *et al.* 1990), methane emission is about 2.5% (Melack *et al.* 2004) and a similar percent is likely to be buried in sediments. The remaining portion is close to being sufficient to fuel the respiration that results in the degassing of 210 ± 60 Tg C y^{-1} as carbon dioxide from rivers and floodplains for this region (Richey *et al.* 2002).

Extrapolating the estimates of aquatic NPP to the whole Amazon Basin is quite difficult. Primary production of these wetlands varies considerably between wetland types and regions from the most productive white-water river floodplains with high

amounts of fertile sediments to clearwater floodplains with intermediate fertility, and black-water rivers with low fertility (Junk *et al.* 2011, Fonseca *et al.* 2019). Large uncertainties stem from the sparseness of measurements and uncertainties in habitat areas. Particularly large data gaps exist for the Llanos de Moxos (Bolivia), peatlands in the Pastaza Marañon foreland basin (Peru, Lähteenoja *et al.* 2012) and central-west Amazon (Lähteenoja *et al.* 2013), coastal freshwater wetlands (Castello *et al.* 2013), riparian zones along streams throughout the basin (Junk *et al.* 2011), small reservoirs associated with agriculture (Macedo *et al.* 2013) and habitats above 500 m. Improved estimates also require incorporation of seasonal and interannual variations in inundation and habitat areas.

Streams and small rivers likely receive almost all the CO_2 released from terrestrial-derived respiration in soils and respiration of organic C from riparian and upland litter as summarized in Richey *et al.* (2009). Inorganic and organic carbon in large rivers is provided by a combination of terrestrial and aquatic carbon sources (with the proportion unknown), and much of this organic carbon is metabolized in rivers (Mayorga *et al.* 2005; Ellis *et al.* 2012; Ward *et al.* 2013, 2016). Photo-oxidation of organic carbon appears to make small contributions to CO_2 in large rivers (Amaral *et al.* 2013, Remington *et al.* 2011).

6.3 Nutrient Cycling in the Amazon Basin

"Nutrient limitation lies at the heart of ecosystem ecology" (Townsend *et al.* 2011). Tropical forests are responsible for about a quarter of global terrestrial NPP, which, in turn, is modulated by the environmental availability of water, energy, and nutrients. Nevertheless, multiple interactions among biogeochemical cycles in multiple nutrients can affect the Amazon C cycle; co-limitation by nitrogen and phosphorus is an important constraint to plant productivity in this system. In general, weathered tropical soils have lower P availability, leading to higher N:P ratios in leaves from tropical forests when compared to high-latitude plants. In contrast, highlighting the diversity of the Amazon

Table 6.1. Annual carbon dioxide fluxes to the atmosphere from aquatic habitats in the Amazon basin including deltaic river channels, coastal freshwater habitats, and Tocantins basin. Basin areas are based on catchment boundaries for river systems, not presence of tropical forest vegetation**.** (These effluxes derive mostly from respiration of carbon produced within aquatic habitats; net fluxes require accounting for hard-to-quantify inputs from aquatic NPP).

Aquatic Habitats	Annual Carbon Dioxide Fluxes
Rivers[1]	137 Tg C y^{-1}
Streams[2]	100 Tg C y^{-1}
Lakes[3]	25 Tg C y^{-1}
Flooded forests[4]	260 Tg C y^{-1}
Other wetlands[5]	200 Tg C y^{-1}
Hydroelectric reservoirs[6]	8.85 Tg C y^{-1}

[1] Channel areas from Allen and Pavelsky (2018) plus L. Hess (personal communication) and Castello *et al.* (2013) for delta, and Sawakuchi *et al.* (2017) for Xingu and Tapajos mouthbays. Fluxes averaged from Richey *et al.* (1990), Rasera *et al.* (2008), Sawakuchi *et al.* (2017), Less *et al.* (2018) and Amaral *et al.* (2019).

[2] Johnson *et al.* (2008) approximated evasion of CO_2 from headwater streams basin wide with a statistical approach that requires validation based on actual measurements in Andean, blackwater and savanna streams.

[3] Open water area of lakes is the difference between total open water area (Hess *et al.*2015) and river channel area (Allen and Pavelsky 2018) guided by lake areas estimated by Sippel *et al.* (1992). Area includes estimates of fringing floating plants. Fluxes averaged from Rudorff *et al.* (2011), Amaral (2017) and Amaral *et al.* (2019).

[4] Floodable forests estimated by Hess *et al.* (2015), and seasonally weighted fluxes derived from Amaral *et al.* (2020).

[5] Aquatic categories lumped as other wetlands (195,000 km^2) include interfluvial wetlands in Negro basin (21,000 km^2), savanna floodplains in Roraima (4,000 km^2), Moxos (35,000 km^2) and Bananal and others in Tocantins basin (35,000 km^2), Marajos Island and other freshwater coastal wetlands (50,000 km^2), and other wetlands scattered throughout the basin (50,000 km^2). Floodable areas from Hess *et al.* (2015), seasonal averages for Roraima, Moxos and Bananal and others in Tocantins basin from Hamilton *et al.* (2002) and Castello *et al.* (2013) plus L. Hess (personal communication). Fluxes for interfluvial wetlands in Negro basin (0.77 Gg C km^{-2} y^{-1}; Belger *et al.* 2011), Roraima (3.5 Gg C km^{-2} y^{-1}; Jati 2014), Pantanal (as surrogate for herbaceous areas in Moxos, Bananal and other wetlands in Tocantins basin; 1 Gg C km^{-2} y^{-1}; Hamilton *et al.* 1995) and estimate for Marajos Island, other freshwater coastal wetlands, and other scattered inundated areas (1 Gg C km^{-2} y^{-1}).

[6] The 159 hydroelectric reservoirs currently in the Amazon basin cover approximately 5350 km^2 (Almeida *et al.* 2019). Hydroelectric reservoirs in the Tocantins basin cover approximately 5,380 km^2. Many are small and the few large ones account for most of the area. In Bolivia (50 km^2), Ecuador (35 km^2) and Peru (103 km^2) almost all are above 1,000 m asl. All in Brazil are in lowlands (<~500 masl; 10,730 km^2) with several in tropical forests and many others in tropical savannas and agricultural landscapes. Very few have adequate sampling to characterize CO_2 emissions. In contrast to methane, almost all evasion to the atmosphere occurs from the reservoir surface with little degassed at the turbines, though some CO_2 generated in the reservoir is emitted downstream (Kemenes *et al.* 2016). The estimation of emissions from Brazilian reservoirs was done in two parts: Average fluxes and areas (total 4,615 km^2) from Kemenes *et al.* (2011) plus slight additional downstream fluxes (Kemenes *et al.* 2016) for Balbina, Samuel, Curua-Una and Tucurui were used to yield 5.7 Tg C y^{-1}. The average value for Amazon reservoirs of 510 g m^{-2} y^{-1}, approximated from Barros *et al.* (2011) was applied to the remaining 6115 km^2 of Brazilian reservoirs to yield 3.1 Tg C y^{-1}. Estimating the emissions from the reservoirs in Bolivia, Ecuador the Peru is more difficult because no measurements exist and at higher elevations temperatures will be lower and the watersheds different from conditions in Brazil. Hence, half the rate applied to the southern Brazilian reservoirs is used to yield an emission of 0.5 Tg C y^{-1}. In total, emissions from hydroelectric reservoirs can be estimated to be approximately 8.85 Tg C y $^{-1}$ with considerable uncertainty and a definite need for many more measurements, especially because more dams are planned. The extent that this estimate represents net emissions, i.e., emissions additional to those associated with the undammed rivers are unknown, but reservoir emissions are likely to be much higher than those in natural rivers.

region, less weathered soils contain a low N:P ratio, potentially making them more limited by nitrogen than by phosphorus (Nardoto *et al.* 2013). Due to the dominance of more weathered soils in the region, model results suggest that taking into account phosphorus limitation may result in a reduction in the NPP response to the increase of CO_2 in the atmosphere (CO_2 fertilization) by up to 50% in the Amazon (Fleischer *et al.* 2019).

6.3.1 Nitrogen

Nitrogen is abundant in Earth's atmosphere in the form of the N_2 molecule, but this stable form is not directly available for biological processes. The conversion of N_2 into reactive forms (e.g., NH_3, NO_X, among others) is essential for life as nitrogen is the foundation for required compounds such as proteins, enzymes, and aminoacids. Within natural ecosystems this conversion is performed by biological nitrogen fixation and, to a much smaller extent, by lightning. Another key process for life and biological functioning is the conversion of organic nitrogen into mineral forms, which are preferable to plants (ammonium [NH_4^+] and nitrate [NO_3^-]). This process, called nitrogen mineralization, is a vital part of soil fertility, and key in terrestrial tropical systems considering the high intensity of organic matter decomposition. Mineralization also leads to N immobilization, when N is incorporated in soil microbial biomass, and to denitrification, the reduction of nitrate (NO_3^-) or nitrite (NO_2^-) into the gases nitric oxide (NO), nitrous oxide (N_2O), or dinitrogen (N_2), with ensuing loss of nitrogen from the ecosystem. Inputs of nitrogen to the Amazon are derived largely from biological nitrogen fixation by microorganisms, which is a process mediated by microorganisms in symbiotic association to specific families of plants and as free-living microorganisms. Other inputs derived from atmospheric deposition are relevant in specific areas of the region.

The abundance of the Fabaceae family in the Amazon forest could indicate the important input of nitrogen through the biological nitrogen fixation (BNF). Some calculations suggested N_2 fixation on

the order of 15 kg N ha^{-1}y^{-1} for ecosystems on Ultisols and Oxisols, and 25 kg N ha^{-1}y^{-1} in more fertile soils (Martinelli *et al.* 2012). However, Nardoto *et al.* (2012) suggested through ^{15}N analysis a low incidence of N_2 fixation by Fabaceae, and the maximum symbiotic fixation rate at the level of 3 kg N ha^{-1}y^{-1} for the Amazon forest. Recent results by Reis *et al.* (2020) suggested BNF rates in South American humid forests are on the order of 10 ± 1 kg N ha^{-1}y^{-1}, where 60% of this total originates from free-living N fixing organisms, and 40% from symbiotic association with legume family plants. These numbers highlight the importance of internal cycling for nitrogen in the Amazon, which is strongly dependent on regular precipitation and soil water availability in the dry season and on the availability of other soil nutrients like phosphorus. Atmospheric wet and dry deposition of reactive nitrogen was estimated to be on the order of 4% of the BNF for the evergreen broadleaf forest in the Amazon (Chen *et al.* 2010). In regions under higher anthropogenic pressure, the rate of reactive nitrogen deposition can be significant; Markewiks *et al.* (2004) found that in Paragominas the N input from precipitation was on the order of 4 kg N ha^{-1}y^{-1}. Internal nitrogen recycling in soil, from undisturbed forests, is the main source of NO and N_2O (see Section 6.4.2) in the Amazon's atmosphere. NO emissions were measured as 4.7 ng N m^{-2}s^{-1} in May 1999 (transition season) and about 4.0 ng N m^{-2}s^{-1} in September 1999 (dry season) in an Amazonian rainforest site in Rondônia (Gut *et al.* 2002a). Davidson *et al.* (2008), analyzing emissions from a water-exclusion experiment in the Tapajós forest in Santarém, reported NO emissions from the control plot (an area without water exclusion) at rates of 0.9 kg N ha^{-1}, as a mean value over five years. However, these emissions do not directly reach the atmosphere above the forest. Some NO is processed within the canopy by oxidation to NO_2 and taken up by plants. Thus, there is a "canopy reduction factor" for NO_X release into the atmosphere (Gut *et al.* 2002b). These ratios can be changed in polluted air from biomass burning, which leads to high NO_X concentrations. Due to the precursor properties of NO_X molecules, ozone (O_3) concentrations also increase. NO_2 concentrations in a rainforest in Ron-

dônia were about three times higher in September/October 1999 then during the wet season in April/May 1999 due to anthropogenic forest fires (Andreae *et al*. 2002). Enhanced NO_x concentrations lead to higher OH concentrations. As OH is the major atmospheric oxidizer, this also strongly affects the oxidation capacity of the atmosphere, which can affect rates of CCN production, cloud formation, and rainfall patterns (Liu *et al*. 2018).

Deforestation and forest regrowth affect soil nutrient cycling and nitrogen dynamics (Figueiredo *et al*. 2019). Chronosequence studies have shown enhanced gross nitrogen mineralization in young regrowing forests followed by a decay which leads to only about half the gross nitrogen mineralization in older regrowth forests compared to the undisturbed forest (Figueiredo *et al*. 2019). Further discussion on secondary forest and land use after deforestation can be found in Chapter 19.

6.3.2 Phosphorus

On the old, weathered soils found in much of the Amazon, it is likely that phosphorus is a more critical limiting macronutrient than nitrogen. Phosphorus plays an essential role in many biological processes such as metabolism and is a building block of DNA, but in natural ecosystems can be very limited. This is primarily because soluble forms of P are found at low concentrations (Markewitz *et al*. 2004, Johnson *et al*. 2001) and gaseous forms are almost non-existent (phosphine [PH_3] being a very rare exception). The effect of low P availability is further exacerbated because many tropical soils can occlude soil P and render it unavailable to plants. The main inputs of P into Amazonian ecosystems are from (i) weathering, either from local soils or from Andean material transported in rivers and deposited in floodplains, and (ii) deposition in the form of dust (e.g., from the Sahara) or ash (from biomass burning). P in biogenic aerosols and from biomass burning represents recycling of P largely within the Amazon system, whereas P deposition from Saharan dust represents a new atmospheric input of P.

The main loss term is export of sediment or organic material via river systems, or through harvesting. Within the basin, lateral movement of P, for example from floodplains rich in Andes-derived sediments, may be facilitated by animals (Doughty *et al*. 2013, Buendía *et al*. 2018); such animal-mediated lateral transfer may have been much stronger in the past prior to megafaunal extinction and more recent defaunation. Total atmospheric deposition of P is estimated to be 16–30 kg P km^{-2} y^{-1} (Vitousek and Sanford 1986), of which Saharan dust inputs are estimated to be no more than 13%, and the bulk is from biogenic aerosols and biomass burning (Mahowald *et al*. 2005). Vitousek and Sanford (1986) estimated that the recycling of phosphorus through litterfall is 140–410 kg P km^{-2} y^{-1}, an order of magnitude greater than atmospheric inputs.

Local weathering inputs are estimated to average 2.5 kg P km^{-2} y^{-1} (Doughty *et al*. 2013). However, weathering rates are variable, and the oxisols that dominate much of the eastern Amazon have virtually no weatherable appatite left, so weathering inputs of P are practically zero. The Amazon Basin experiences continental isostatic rebound, where the slow erosion rates are compensated by slow uplift and weathering of new material (Buendía *et al*. 2018). For the area of the Amazon Basin (including the Guyanas), total P inputs are ~2.8 Tg C y^{-1}. Fluvial export of P, based on discharge at Óbidos, is 1.46 Tg P y^{-1}, about half of the inputs to the basin (Devol *et al*. 1991).

There are strong gradients in P availability across the basin, with the lowest availability on old, weathered oxisols of the eastern Amazon, and higher concentrations on younger soils in the western Amazon (Aragão *et al*. 2009, Quesada *et al*. 2010). The high productivity of the Amazon forest, despite this low P availability, is facilitated by very tight recycling of P within the forest system, where around half of leaf P is either resorbed prior to leaf senescence, and most of the rest is rapidly captured by fungal hyphae soon after litter fall or plant death (Cuevas and Medina 1986, Markewitz *et al*. 2004).

6.4 Other Major Greenhouse Gases

6.4.1 Methane

6.4.1.1. Terrestrial Methane Fluxes

Methane is a strong greenhouse gas due its importance in radiative forcing, contributing to climate change and with a warming potential relative to CO_2 of 28-34 for a 100-year time horizon. In addition, methane is the primary anthropogenic volatile organic compound (VOC) in the global troposphere (Fiore *et al*. 2002), contributing to tropospheric O_3 formation by photochemical reactions (West *et al*. 2006). In the stratosphere, methane reacts with chlorine atoms, which is a stratospheric ozone-depleter (Cicerone 1987). Methane is produced by different processes (i.e., biogenic, thermogenic, or pyrogenic), can be of anthropogenic or natural origin, and is consumed by a few sinks. The balance between sources and sinks determines the methane budget. In terrestrial environments, anoxia in soil leads to the production of methane as a terminal step in the degradation of organic matter by anaerobic methanogenic archaea. Methanotrophs in terrestrial soils can consume methane under aerobic conditions. The balance between the two processes is regulated by climatic and edaphic factors, such as soil temperature, oxygen content, soil pH, water table, and electron acceptors (Conrad 2009).

Well-drained soils of the Amazonian upland forest are often a net CH_4 sink, estimated to be 1-3 Tg CH_4 y^{-1} (Davidson and Artaxo 2004, Dutaur and Verchot 2007). However, rainfall, poor drainage, and soil properties can create localized anoxic microsites that can facilitate methane production, causing forests to switch from sinks to small sources (Verchot *et al*. 2000). Oxygen availability in forest soils is known to influence methane production, with emissions of 0.5-2.3 mg of CH_4 $m^{-2}d^{-1}$ observed in a montane forest in Puerto Rico (Teh *et al*. 2005). Anaerobic decay of waterlogged wood (Zeikus and Ward 1974) and deadwood (Covey *et al*. 2016) are also sources of methane. Methane can be produced by a variety of fungi and archaea within tree stems,

a process identified by Zeikus and Ward (1974) and now recognized as common and perhaps present in living trees with no visual decay (Covey & Megonigal 2018).

Methane sources have been detected within forest canopies (Carmo *et al*. 2006). Tank bromeliads (Martinson *et al*. 2010) and termites (Martius *et al*. 1993) are known to produce methane and also harbor methanogens. Large, site specific emissions from termites (25.9 ± 11.2 mg CH_4 g termite^{-1} y^{-1}; Martius *et al*. 1993) and tank bromeliads (3.6 g CH_4 ha^{-1} d^{-1}; Ecuadorian Andes, Martinson *et al*. 2010) have been reported. A recent study in the Amazon found high emissions from mounds of soil feeding termites ranging from 3.5-16.4 µg CH_4 m^{-2} d^{-1}, suggesting the role of termites is likely underestimated at an ecosystems scale (van Asperen *et al*. 2020). Epiphytic bryophytes on tree stems and branches can act as sources and sinks of methane, as indicated by two studies in non-Amazonian forests (Lenhart *et al*. 2015, Machacova *et al*. 2017). These methane sources within canopies are highly heterogeneous with limited measurements, hence, it is difficult to estimate their regional strength.

Methane can be produced by a novel abiotic pathway from plant tissues, with an estimated global source strength of up to 1 Tg CH_4 y^{-1} (Bloom *et al*. 2010). Reactive oxygen species in plant tissues commonly produced in response to plant stress are known to drive these abiotic methane emissions. Upland tree stem and leaf surfaces are postulated to offer additional terrestrial sinks (Covey and Megonigal 2018); however, direct observations are presently lacking.

Anthropogenic activities in terrestrial ecosystems can both emit or take up methane. Briefly, land use changes such as logging or conversion of forests to agriculture reduce the capacity of the soil methane sink due to soil compaction (Bustamante *et al*. 2009). Forest fire is known to emit methane in the short term (Wilson *et al*. 2016), reduce the methane sink in some forests, and reduce methane emissions from wetland trees in flooded forests initially, but later may result in enhanced emissions

due to the increased availability of substrates for methanogenesis. Land conversion to animal farming with the introduction of ruminant livestock increases emissions due to enteric fermentation. Waste management and direct production during biomass burning increases methane emissions. Land conversion following river damming changes the flooding regime both upstream and downstream and are documented to increase methane emissions (see next section).

6.4.1.2. Freshwater Methane Fluxes

Methane emission to the atmosphere from aquatic environments (Table 6.2) reflects differences between CH_4 production by methanogens, mainly in anoxic sediments, and consumption by methanotrophs, as well as physical processes. These processes are influenced by environmental variables such as water temperature, dissolved oxygen, trophic status, and substrate availability. CH_4 can reach the atmosphere by three pathways: via diffusive fluxes at the air-water interface; via bubbles that form in the sediment, rise through the water column, and are emitted to the atmosphere (ebullition); and through the vascular systems of herbaceous and woody plants. Wetland-adapted trees are known to transport and emit soil-produced methane to the atmosphere via tree trunk and leaf surfaces (Pangala *et al.* 2017). Ebullitive fluxes depend on bubble formation and hydrostatic pressure over the sediment, while diffusive fluxes are dependent on concentration gradients and turbulence, which vary on multiple time and spatial scales. Factors such as wind speed, diel variation in thermal structure, and physical processes such as convective and advective mixing are all known to influence gas distributions and transfer velocities, and consequently gas fluxes.

Table 2 summarizes methane fluxes from major aquatic environments in the Amazon Basin. Fluxes of methane from all aquatic environments within the catchments of the Amazon and Tocantins river systems, covering 970,500 km^2, are estimated to be approximately 51 Tg CH_4 y^{-1}. Given the varied approaches and associated uncertainties in these

values, the procedure used for each category is described briefly – including both the area of each category and the average annual flux per km^2, based on selected studies with the most comprehensive or representative data, where possible.

River channel areas (85,500 km^2) are based on Allen and Pavelsky (2018) plus L. Hess (personal communication) and Castello *et al.* (2013) for the delta, and Sawakuchi *et al.* (2017) for the Xingu and Tapajos mouthbays. Average fluxes (8 Mg CH_4 km^{-2} y^{-1}) are from Sawakuchi *et al.* (2014) and Barbosa *et al.* (2016). Stream channel area (50,000 km^2) is estimated from geomorphological features (Richey *et al.* 2002, Beighley and Gummadi 2001), and average fluxes (6.6 Mg CH_4 km^{-2} y^{-1}) for tropical and subtropical streams are from Stanley *et al.* (2016). Open water area of lakes is the difference between total open water area (Hess *et al.* 2015) and river channel area (Allen & Pavelsky 2018) guided by lake area estimates by Sippel *et al.* (1992). Lake area includes estimates of areas with floating plants. Fluxes are averaged from Barbosa *et al.* (2020). Floodable forest area (615,000 km^2) is derived from Melack & Hess (2010) and Hess *et al.* (2015). Seasonally weighted fluxes from water surfaces under flooded forests (26.6 Mg CH_4 km^{-2} y^{-1}) are derived from Barbosa *et al.* (2020), Barbosa *et al.* (2021) for *várzea*, and from Rosenqvist *et al.* (2002) for *igapó*. Fluxes through trees in flooded forests are estimated to be 21.2 ± 2.5 Tg CH_4 y^{-1}; forested wetland soils are responsible for an additional 1.1 ± 0.7 Tg CH_4 y^{-1} (Pangala *et al.* 2017).

Aquatic categories lumped as other wetlands (195,000 km^2) include interfluvial wetlands in the Rio Negro Basin (21,000 km^2); savanna floodplains in Roraima (4,000 km^2), Moxos (35,000 km^2), Bananal, and others in the Tocantins Basin (35,000 km^2); Marajos Island and other freshwater coastal wetlands (50,000 km^2); and other wetlands scattered throughout the basin (50,000 km^2). Floodable areas are based on Hess *et al.* (2015); seasonal averages for Roraima, Moxos, Bananal, and others in the Tocantins Basin are from Hamilton *et al.* (2002) and Castello *et al.* (2013), plus L. Hess (personal communication). Fluxes are estimated as follows:

interfluvial wetlands in the Rio Negro Basin 28 Mg CH_4 km^{-2} y^{-1} (Belger *et al.* 2011), Roraima 5.3 Mg CH_4 km^{-2} y^{-1} (Jati 2014), Pantanal, as a surrogate for herbaceous areas in Moxos and elsewhere) 80 Mg CH_4 km^{-2} y^{-1} (Hamilton *et al.* 1995), and estimates for Marajos Island and other freshwater coastal wetlands (27 Mg C km^{-2} y^{-1}).

Hydroelectric reservoirs (158) in the Amazon Basin currently cover approximately 5,350 km^2 (Almeida *et al.* 2019; see footnotes in Table 6.2). Hydroelectric reservoirs in the Tocantins Basin cover approximately 5,380 km^2. Very few have adequate sampling to characterize methane emissions. One example is Balbina, where measurements over a year were made of diffusive and ebullitive fluxes from multiple stations within the reservoir, degassing at the turbines and downstream (Kemenes *et al.* 2007). Another example is the multiyear study at Petit Saut (French Guiana) that included measurements in the reservoir and downstream (Abril *et al.* 2005). Both these studies indicate the importance of degassing of methane through the turbines and downstream. Additional measurements at Tucurui, Samuel, and Curua-Una reservoirs indicated the significance of degassing at the turbines and downstream (Kemenes *et al.* 2016). Extrapolating all emissions based on reservoir areas combined with turbine and downstream emissions yields a total of 0.4 Tg CH_4 y^{-1} for Balbina, Curua-Una, Samuel, and Tucurui. To estimate emissions from the other Brazilian reservoirs, an overall average diffusive and ebullitive emission from the surfaces of ten reservoirs within southern portions of the basin (~29 g CH_4 m^{-2} y^{-1}, as summarized in Deemer *et al.* 2016) and the combined surface areas of all the additional Brazilian reservoirs yields 0.18 Tg CH_4 y^{-1}.

Estimating emissions from reservoirs in Bolivia, Ecuador, and Peru is more difficult because no measurements exist and at higher elevations temperatures will be less and the watersheds different from conditions in Brazil. Hence, half the rate applied to the southern Brazilian reservoirs is used to yield an emission of ~0.002 Tg CH_4 y^{-1}. In total, methane emissions from hydroelectric reservoirs can

Table 6.2. Annual methane fluxes to the atmosphere from aquatic habitats in the Amazon basin including deltaic river channels, coastal freshwater habitats and Tocantins basin plus hydroelectric reservoirs.

Aquatic Habitats	Annual Methane Fluxes
Rivers	0.7 Tg CH_4 y^{-1}
Streams	0.4 Tg CH_4 y^{-1}
Lakes	0.7 Tg CH_4 y^{-1}
Flooded forests	
Flux from water surface	16.4 Tg CH_4 y^{-1}
Flux through trees	21.2 Tg CH_4 y^{-1}
Flux from exposed soil	1.1 Tg CH_4 y^{-1}
Other wetlands	9.6 Tg CH_4 y^{-1}
Hydroelectric reservoirs	0.58 Tg CH_4 y^{-1}

be estimated to be approximately 0.58 Tg CH_4 y^{-1} (Table 6.2) with considerable uncertainty and a definite need for many more measurements, including degassing through turbines and downstream, especially because more dams are planned. The extent that this estimate represents net emissions, i.e., emissions additional to those associated with the undammed rivers, are unknown, though upland forest soils are likely to be sinks for methane.

As noted in Section 6.2.2, large uncertainties stem from the sparseness of measurements of fluxes and uncertainties in habitat areas and their seasonal and interannual variations. Temporal differences in methane fluxes are owed to variations in inundation as a result of differences in river discharge, local runoff and rainfall, related ecological conditions, and changes in areal coverage of different habitats. Multi-year time-series of measurements are not available to document possible trends or variations. Current hydrological models provide estimates of variations in inundation, but underestimate basin-wide conditions. Remote

sensing products include inundated areas, though the longest time-series under-estimate areas in some habitats and have moderate spatial resolution; high resolution products are temporally sparse. Distinguishing among the varied aquatic habitats relies on a combination of optical and microwave products which lack sufficient time-series.

6.4.1.3. Amazon Methane Budget

Both bottom up and top-down estimates with different spatial and temporal scales are available for the Amazon Basin. Bergamaschi *et al.* (2009) used SCIAMACHY data to calculate total Amazon emissions of 47.5 to 53.0 Tg CH_4 y^{-1} in 2004 for an area of 8.6×10^6 km^2. Based on an inversion model using *in situ* and remote sensing observations, Fraser *et al.* (2014) estimated emissions of 59.0 ± 3.1 Tg CH_4 y^{-1} from tropical South America (approximately ~9.7×10^6 km^2) in 2010. Tunnicliffe *et al.* (2020) using inverse modelling estimates derived from GOSAT satellite measurements combined with surface data, and the high-resolution regional atmospheric transport model NAME, reported mean emissions for wetlands in the Brazilian Amazon substantially lower than other estimates (9.2 ± 1.8 Tg CH_4 y^{-1}). Wilson *et al.* (2016) performed an inversion with the TOMCAT model using aircraft vertical profile observations and estimated methane emissions of 36.5 to 41.1 Tg CH_4 y^{-1} in 2010 and 31.6 to 38.8 Tg CH_4 y^{-1} in 2011 (area of 5.8×10^6 km^2), with non-combustion emissions representing 92-98% of total emissions. Pangala *et al.* (2017) provide a regional estimate of methane emissions of 42.7 ± 5.6 Tg CH_4 y^{-1} (area of 6.77×10^6 km^2) based on regular vertical lower troposphere profiles covering the period 2010–2013, where 10% came from biomass burning. This estimate is similar to bottom-up estimates for the same area. Estimates of total methane fluxes based on aircraft vertical profiles measurements for the northeastern Amazon ($2.8°S$, $54.9°W$; considering an area of 0.6×10^6 km^2) are between 7.5 and 11.7 Tg CH_4 y^{-1} (Miller *et al.* 2007, Basso *et al.* 2016, Pangala *et al.* 2017), where natural sources, like wetlands, are likely important, with biomass burning representing almost 10% of total annual mean flux and anthropogenic emissions representing around 11% of the annual mean flux (Basso *et al.* 2016). This region has higher fluxes than other regions (Wilson *et al.* 2016, Pangala *et al.* 2017), which highlights regional variability in methane emissions in the Amazon.

The overall methane budget includes multiple sources and sinks whose contributions are sensitive to feedback from drought conditions, and significant gaps remain in understanding how droughts will affect methane budgets (Saito *et al.* 2016). During the 2010 drought, methane emissions from biomass burning were around 5-6 times higher than 2011, varying from 0.5 to 7.0 Tg CH_4 y^{-1} depending on the climate condition (drought years), which part of the Amazon was being considered, and the severity of the burn season (Wilson *et al.* 2016, Saito *et al.* 2016).

Top-down estimates of methane emissions indicate that the Amazon is an important source; extrapolating these estimates for the same area (an Amazon area of 6.77×10^6 km^2) total methane emissions vary between 36.9 and 48.0 Tg CH_4 y^{-1} (Bergamaschi *et al.* 2009, Fraser *et al.* 2014, Wilson *et al.* 2016, Pangala *et al.* 2017). This suggests the region contributes 6-8% of global methane emissions, considering global emissions of 576 Tg CH_4 y^{-1} (Saunois *et al.* 2020).

6.4.2 Nitrous Oxide (N_2O)

6.4.2.1 Terrestrial Biosphere N_2O Processes

Nitrous oxide (N_2O) is, after carbon dioxide (CO_2) and methane (CH_4), the third most important long-lived greenhouse gas, and one of the main stratospheric ozone depleting substances. The majority of anthropogenic N_2O is produced by the agricultural sector, although natural systems emit nitrous oxide via organic matter decomposition processes, particularly in the soil. Emissions of N_2O, predominantly from denitrification, are related to biological and physical-chemical characteristics of the soil. Soil microbial processes modulate organic

matter mineralization and environmental conditions such as soil water content, N availability, soil texture, pH, and labile organic carbon content are important conditions for the transformation of organic matter and dissolved nutrients to plants and soil biota. Rapid nutrient cycling related to higher temperatures, water availability, and high N:P ratios result in tropical forests emitting high rates of N_2O to the atmosphere. Tropical regions account for 71% of global natural ecosystem emissions (Yu and Zhuang 2019). Ciais *et al.* (2014) reported global N_2O emissions from natural vegetation of 6.6 Tg N y^{-1} (ranging from 3.3 to 9.0 Tg N y^{-1}, IPCC AR5). Recently, Tian *et al.* (2020) reported global emissions from natural soils (with strong contributions from the tropics) in the period from 2007-2016 on the order of 4.9 to 6.5 TgN y^{-1}. Syakila and Kroeze (2011) simulated an increase of 8 times, of total anthropogenic N_2O emissions, from the beginning of the industrial revolution to 2006, from 1.1 TgN y^{-1}, in 1850 to 8.3 Tg N y^{-1} in 2006, with the emissions from global natural systems maintained at 10.5 Tg N y^{-1}. Over the same period, the global N_2O Model Intercomparison Project (NMIP) simulations (from 1860 onwards) indicate the highest N_2O global emissions derived from tropical areas, and tropical South America (particularly the Amazon region), accounting for 20% of global emissions (Tian *et al.* 2018). The models consider natural and human transformed land use (e.g., agriculture, pasture) in the simulations.

6.4.2.2. Freshwater Biosphere N_2O Processes

Most N_2O emissions from freshwater systems occur in wetlands. Guilhen *et al.* (2020), in a study of the wetlands along the Amazon, Madeira, and Branco rivers, circa 1.3 x 10^6 km^2, modelled N_2O emissions from denitrification on the order of 1.8 kg N_2O $ha^{-1}y^{-1}$, peaking in March. Total emissions from denitrification in the Amazon Basin floodplains are estimated to be 1.03 Tg N- N_2O y^{-1}. Due to the abundance of nitrogen in Amazonian soils, nitrate may not be limiting denitrification in the Amazon Basin (Guilhen *et al.* 2020).

6.4.2.3. The Amazon N_2O Budget

Estimates for N_2O emissions in tropical forest soils ranged from 0.8 Tg N y^{-1} (mean for 1991–2000) for South America (Felipe Pacheco and INMS, personal communication) to 2.40 Tg N y^{-1} (Matson and Vitousek 1990) and 3.55 Tg N y^{-1} (Breuer *et al.* 2000) for tropical humid forests globally. Melillo *et al.* (2001) and Davidson *et al.* (2001) calculated emissions from the Amazon tropical forest of 1.2 to 1.3 Tg N y^{-1}. Buscardo *et al.* (2016) estimated the highest N_2O emissions in the north-west portion of the basin, decreasing with drier conditions towards the east and south, with an average estimate of 0.74 to 0.83 Tg N y^{-1} for the entire Amazon Basin. Variation was due to the fraction attributed to soil respiration. Figueiredo *et al.* (2019) and Galford el al. (2010) suggest that the Amazon's mature forests (including *terra firme* and periodically flooded forests) are responsible for circa of 6.5% of global N_2O emissions from natural systems, and fluxes are estimated on the order of 0.5-2.5 kg N ha^{-1} (Lent *et al.* 2015, Tian *et al.* 2020). In a comprehensive review conducted by Meurer *et al.* (2016) it was shown that the median annual flux rates from Amazonian forests were about 36% higher than the N_2O fluxes rates from the Atlantic rainforest (2.42 and 0.88 kg N ha^{-1}, respectively). Land use change significantly alters the emissions of N_2O. Due to increased soil N availability, when pasture replaces the forest, fluxes may double or triple, but then decrease in the years following conversion to less than half of the original emissions (Davidson *et al.* 2007). Biomass burning is currently responsible for about 0.7 Tg N y^{-1} emission of N_2O (Davidson and Kanter 2014). In agricultural systems in the Amazon region, double cropping is important, with soy-maize and soy-cotton the most common rotation. Soy fixes nitrogen at a rate of 200 kg ha^{-1}, but N_2O emissions are fairly low, 0.1-0.2 kg ha^{-1} (Cruvinel *et al.* 2011). The following crop, with the addition of mineral fertilizer, emits N_2O on the order of 0.2 to 0.8 kg ha^{-1}, depending on the amount of fertilizer used (Jankowski *et al.* 2018). Regional N_2O emissions from natural ecosystems are presented in Figure 6.6.

6.5 Aerosols and Trace Gases

6.5.1 Biogenic Non-Methane Volatile Organic Compounds (NMVOCs)

The Amazonian ecosystem is regarded as the largest source of biogenic Non-Methane Volatile Organic Compounds (NMVOCs), also known as biogenic volatile organic compounds (BVOCs) (Figure 6.7). Emissions of NMVOCs make a minor contribution to the carbon cycle (Figure 6.2, Kesselmeier *et al.* 2002). Biogenic NMVOCs are characterized by their high chemical reactivities and thus represent key players in oxidation processes in the atmosphere (Williams *et al.* 2016, Nölscher *et al.* 2016, Pfannerstill *et al.* 2018). They affect atmospheric chemistry and physics in major ways, by changing the oxidation capacity and particle production, and delivering so-called secondary organic aerosols (SOA) which add to the effects of primary biological particles in the atmosphere. Anthropogenic effects as well as climate and global change have severe effects on NMVOC emission rates (Peñuelas and Staudt 2010, Liu *et al.* 2016) and affect particle production, with consequences for water condensation, cloud production, and the water cycle.

Of significance is the heterogeneity of VOC emissions from vegetation and the dynamics of seasonal or developmental changes in the Amazon (Yáñez-Serrano *et al.* 2015, 2020). With increasing understanding of biogeochemical cycles and atmospheric reactivity, there is growing interest in the large group of biogenic NMVOCs, which represent the dominant source of organic volatiles in the atmosphere, especially in forest dominated areas. Biogenic production and release of NMVOCs are closely related to plant biodiversity and, consequently, the number of biogenic volatiles is enormous (Kesselmeier and Staudt 1999, Laothawornkitkul *et al.* 2009). In line with their large numbers, their roles are still a matter of discussion in view of ecology and chemistry. In particular, the complex composition of BVOCs, including oxygenated species, aromatic compounds, sulfurous compounds, oxidation products, and further unknown reactive compounds leaves questions about atmospheric reactivity (Kesselmeier and Staudt 1999, Nölscher *et al.* 2016, Pfannerstill *et al.* 2018, Yáñez-Serrano *et al.* 2018).

NMVOC research in the Amazon. Field locations such as the Amazonian Tall Tower Observatory (ATTO) can contribute to this research (Andreae *et al.* 2015). Complications arise from deforestation, which changes the diversity of volatiles and thus chemical reactivity. The loss of forested areas will affect not only the carbon cycle but also NMVOC exchange between the surface and the atmosphere, particle production, and the water cycle. Furthermore, the influence of fires on particle numbers are impressive, when comparing the dry season (with fire) to the wet season (without fires) (Andreae 2019, Pöhlker *et al.* 2019). Conversely, direct SOA contributions from fire emissions seems to be low when analyzing Mediterranean fires (Bessagnet *et al.* 2008). Significant gaps in understanding the emission regulation and fate of emitted NMVOCs remain. Major unknowns with potential impact are the emission capacity and quality of flooded areas, the role of root anoxia (Bracho-Nunez *et al.* 2012), and ecological interactions within the forest (Salazar *et al.* 2018).

6.5.2 Physics and Chemistry of Aerosols and Cloud Condensation Nuclei (CCN)

Besides influencing water and nutrient cycles, aerosols affect radiation directly by light scattering and absorption as well as indirectly by cloud condensation and processing. Under natural conditions, the Amazon is one of the few continental regions where aerosol concentrations resemble those of the pre-industrial era, in the range of 300-500 particles per cm^3 and 9-12 $\mu g/m^3$ (Andreae 2007, Martin *et al.* 2010). Organic carbon dominates the composition of submicrometer aerosols in the Amazon in the wet season, comprising about 70% of mass, followed by sulfate (10-15%) and equivalent black carbon (5-10%) (Andreae *et al.* 2015, Chen *et al.* 2015). Observations indicate that about 90% of submicron organic aerosol mass results from secondary production (Chen *et al.* 2009). Oxidation of BVOCs by O_3 and OH leads to the formation of semivolatile organic species, with sufficiently low vapor pressure to condense over pre-existent particles and produce secondary organic aerosols (SOA) (Graham *et al.* 2003, Pöhlker *et al.* 2012). Another pathway for the production of SOA from BVOC emissions consist of aqueous-phase
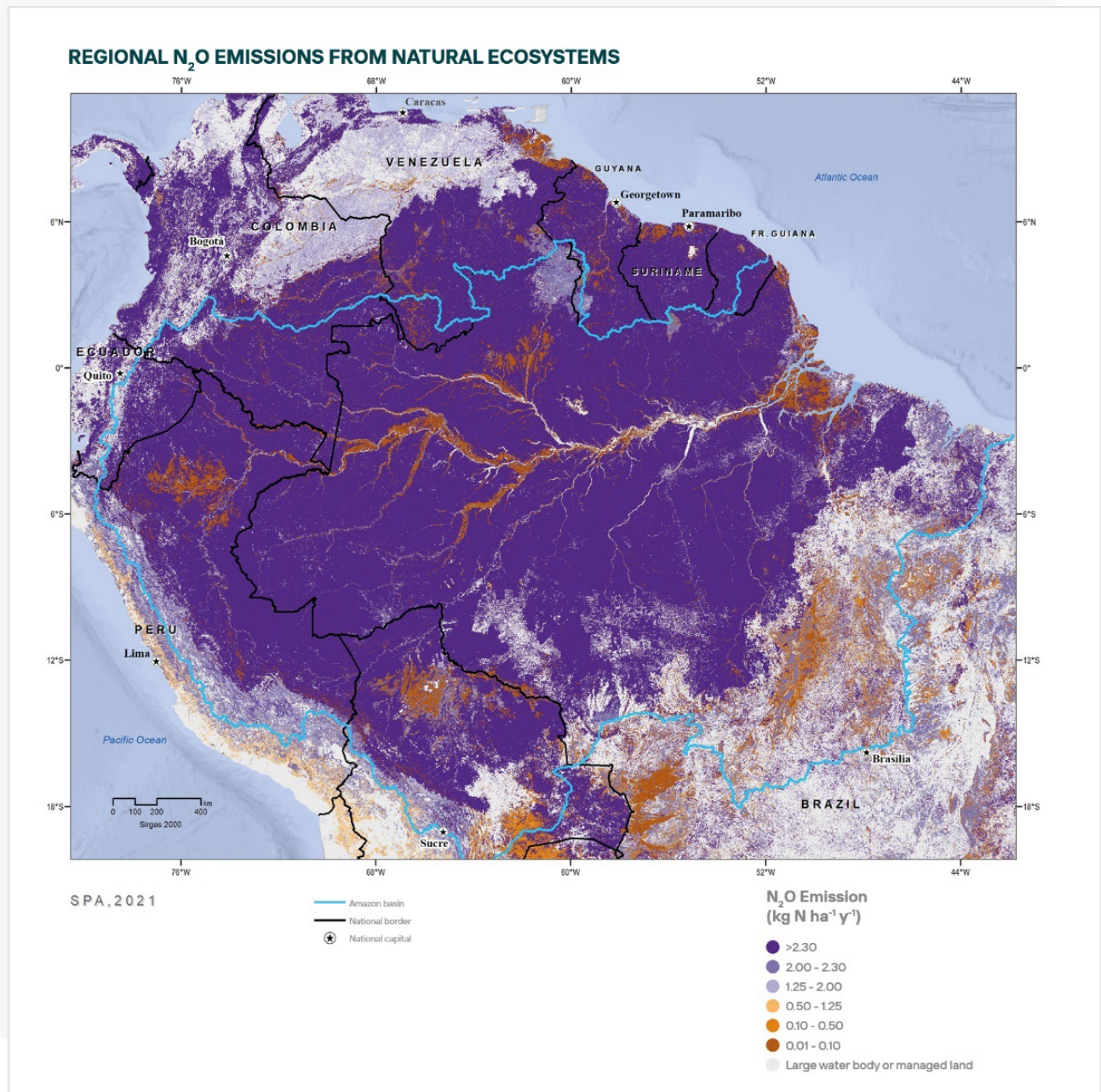
REGIONAL N₂O EMISSIONS FROM NATURAL ECOSYSTEMS

Figure 6.6 N$_2$O emissions in the Amazon. Data produced by Felipe Pacheco, based on data and analysis from the International Nitrogen Management Assessment (INMS).
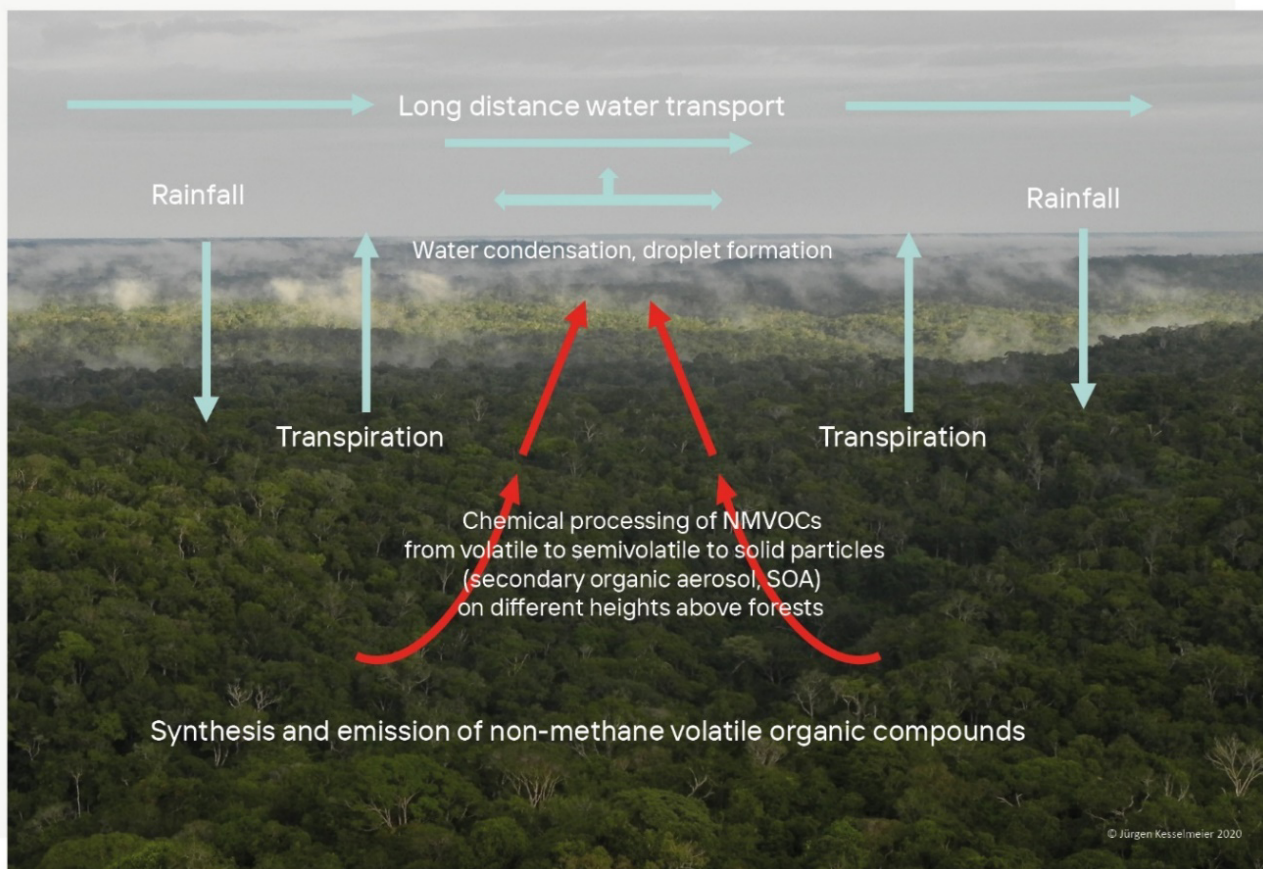
Figure 6.7 The NMVOC emissions of the Amazonian rainforest act as a water catching and water transporting organic system by chemical and physical processing of biogenic trace gases to secondary organic aerosol serving as condensation nuclei for water vapor.

oxidation and acid-catalyzed reactive uptake of isoprene oxidation products within cloud and fog droplets (Lim *et al.* 2010, Surratt *et al.* 2010). Characterization of submicrometer organic aerosols in a forest site in the Amazon suggests comparable importance of aqueous and gas-phase pathways of SOA production (Chen *et al.* 2015).

Another mechanism of SOA production is new particle formation (NPF) in the diameter range <10 nm, followed by condensational growth to the accumulation mode (~100-300 nm). This process has been demonstrated to be a relevant source of particles in boreal forests (Dal Maso *et al.* 2005). However, the impact of NMVOC on particle production over the Amazon is surprisingly different from

what occurs in temperate and boreal forests (Andreae *et al.* 2018, Artaxo *et al.*, in review). Long-term observations at Amazonian forest sites have shown that regional-scale NPF events are infrequent near the surface (3% of measurement days) (Rizzo *et al.* 2018). Instead, airborne measurements in the Amazon reported high concentrations of nucleation and Aitken mode particles (diameter <~100 nm) in the upper troposphere. A conceptual model was developed to describe this important source of particles in the Amazon (Figure 6.8). BVOCs emitted at the vegetation canopy surface are transported upward inside convective clouds to the upper troposphere, where they experience the ideal conditions for particle nucleation (high actinic flux, low temperatures, and small condensation sink). SOA are
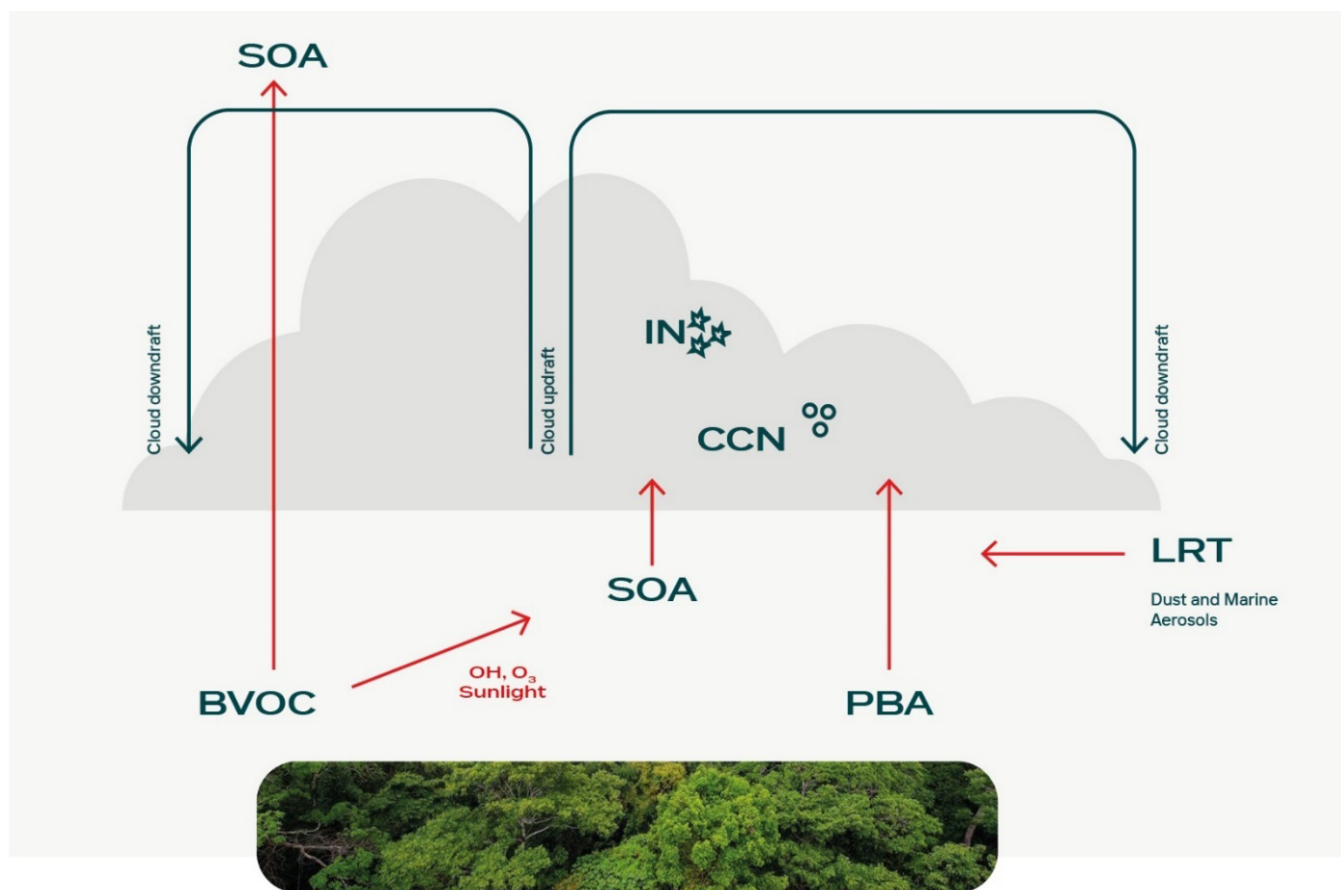
Figure 6.8. Interactions between biogenic emissions, long range transport (LRT) of aerosols and clouds in Amazon. Biogenic volatile organic compounds (BVOCs) are oxidized near the surface, leading to the production of secondary organic aerosols (SOA). Primary biological aerosols (PBA), SOA and LRT aerosols activate into cloud condensation nuclei (CCN) and ice nuclei (IN), promoting the development of clouds and precipitation. BVOCs are transported by convective updrafts to the upper troposphere, where ideal conditions for particle nucleation are found. SOA are produced from BVOC oxidation in the upper troposphere and are eventually transported to the surface by convective downdrafts, constituting an important natural source of particles.

produced from BVOC oxidation in the upper troposphere and are eventually transported to the surface by convective downdrafts, increasing in size by condensation on the way down (Andreae *et al.* 2018, Wang *et al.* 2016).

In the Amazon forest, coarse mode aerosols (diameter >2.5 µm) dominate the mass size spectra during the wet season, including primary biological aerosols (PBA), marine aerosols, and long-range transported (LRT) African aerosols (Andreae *et al.* 2015, Martin *et al.* 2010, Moran-Zuloaga *et al.* 2018). Pollen, bacteria, spores, and fragments of biological material are examples of PBA emitted in the Amazon forest (China *et al.* 2016, Huffman *et al.* 2012,

Pöhlker *et al.* 2012). LRT of aerosols from Africa is typically observed in the Amazon between December and April, consisting of Saharan dust and biomass burning aerosols from the Sahel region (Baars *et al.* 2011, Pöhlker *et al.* 2019, Saturno *et al.* 2018). LRT episodes are relatively frequent in the wet season (5 to 10 events per year), usually lasting from 3 to 10 days (Moran-Zuloaga *et al.* 2018, Rizzolo *et al.* 2017). During LRT episodes, concentration enhancements on aerosol mass, equivalent black carbon, crustal elements (Al, Si, Ti, Fe), and potassium are observed, providing key nutrients for Amazonian ecosystems (Martin *et al.* 2010, Moran-Zuloaga *et al.* 2018, Rizzolo *et al.* 2017, Saturno *et al.* 2018).

Aerosol particles constitute an essential ingredient for cloud formation and development, since they can act as cloud condensation nuclei (CCN), over which water vapor condenses, producing cloud droplets. Moreover, some particles, known as ice nuclei (IN), can initiate the formation of ice crystals inside clouds, providing faster growth to precipitable droplet sizes when compared to CCN, and thus influencing precipitation (Andreae and Rosenfeld 2008). Measurements and modelling indicate that biogenic SOA act as CCN in the Amazon forest, while IN consist of coarse mode PBA and LRT mineral dust particles from Africa. In addition, coarse mode aerosols can act as giant CCN, generating large droplets and inducing rain in warm clouds (Pöhlker *et al.* 2016, 2018; Pöschl *et al.* 2010; Prenni *et al.* 2009). While aerosols provide nuclei for cloud formation, convective clouds may stimulate the formation of SOA particles through in-cloud processing of biogenic emissions (Figure 6.8), making an intrinsic connection between aerosol and cloud processes. An ensemble of observations demonstrates the biosphere-atmosphere integration in the Amazon, joining biogenic emissions, clouds, and precipitation, depicting the forest as a biogeochemical reactor. The biosphere emits BVOCs and aerosols, which are processed by photochemistry, providing nuclei for the formation of warm and cold clouds, which result in precipitation, sustaining the hydrological cycle and biological reproduction, closing a virtuous cycle (Pöhlker *et al.* 2012, Pöschl *et al.* 2010).

6.5.3 Ozone and Photochemistry

Ozone (O_3) is a highly reactive trace gas, with largely varying atmospheric concentrations globally. There is no significant direct source of tropospheric O_3; therefore, its concentration strongly depends on precursors like NO_X, CO, and VOCs (Rummel *et al.* 2007, Yáñez-Serrano *et al.* 2015, Lu *et al.* 2019) and to a smaller extent on the exchange between the stratosphere and troposphere (Ancellet *et al.* 1994, Hu *et al.* 2010). Lifetime of O_3 depends on atmospheric chemistry, which is controlled by temperature and radiation. The globally-averaged lifetime of tropospheric O_3 is approximately 23

days (Young *et al.* 2013), but due to surface deposition and chemical reactions it is much shorter in the boundary layer (Cooper *et al.* 2014), which can lead to strong gradients between a well-mixed boundary layer far from strong precursor emission sources and the free troposphere. Concentrations above the oceans or at remote, undisturbed continental areas are significantly lower than those of the surroundings of cities and burning biomass. Hence, the remote Amazon rainforest has turned out to be an ideal place to study O_3 chemistry under nearly pristine conditions. This property has drastically changed due to increased biomass burning and deforestation, which leads to strongly enhanced NO_X and O_3 concentrations over most parts of the Amazon Basin, especially during the drier season between July and October. The strongest sink of O_3 is dry deposition, which can occur through stomatal and nonstomatal uptake by leaves. Soil and water surfaces can additionally act as O_3 sinks (Clifton *et al.* 2020). Analyses of turbulence transport of tropospheric air into the forest combined with O_3 flux measurements can improve the evaluation of these processes. Mixing ratios of O_3 above 40 ppb, which also occur in the remote Amazon due to biomass burning, are known to cause damage to leaves (Pacifico *et al.* 2015) due to generation of reactive oxygen species that can induce cell death and lesions (Clifton *et al.* 2020). Hence, even remote areas far away from biomass burning can be very negatively affected by air pollution transported over several hundreds of kilometers.

6.6 Conclusions

The Amazon is a key feature of the planetary biosphere; its biogeochemical cycles are major factors for the environment and climate, and form the largest single-biome contribution to many key planetary biogeochemical processes. Geological and climatic variability across the Amazon plays an important role in shaping the features of the region's biogeochemistry and ecosystem functions. The exchange of trace gases, such as greenhouse gases and reactive gases, and secondary and primary particles, contribute directly and/or indi-

rectly to the greenhouse effect and affect atmospheric chemistry and physics. Emission (production) and deposition (uptake) processes affect the current concentration of greenhouse gases such as methane, carbon dioxide, ozone, and nitrous oxide. Reactive trace gases affect the oxidative capacity of the atmosphere with significant influences on particle production and cloud condensation processes. Hence, climate is affected at local, regional, and global scales, including atmospheric warming, chemical processing in the atmosphere, and hydrology. Continued degradation of the Amazonian rainforest and passing of tipping points would result in a weakening and potential collapse of the biogeochemical network reaching from the soil and forest up to the atmosphere. This would have severe consequences for Amazonian ecosystems and for the communities that rely on them.

6.7 Recommendations

- There is a need to better understand and create an early warning system for the stability of the Amazon carbon store and sink in light of global environment change. Loss or reversal of the Amazon carbon sink would have global consequences and make it more difficult to limit peak warming to the internationally-agreed target of 1.5°C or 2°C.
- There is a need to better quantify and map the sources and sinks of methane and N_2O in the Amazon system.
- The potential role of the Amazon biome and its associated atmospheric chemistry in influencing cloud properties and regional and global climate needs to be better quantified and may be amongst the most significant contributions of the Amazon to planetary function.

6.8 References

Abril G, Guérin F, Richard S, et al. 2005. Carbon dioxide and methane emissions and the carbon budget of a 10-year old tropical reservoir (Petit Saut, French Guiana). *Global Biogeochem Cycles* **19**: GB4007.

Albert LP, Restrepo-Coupe N, Smith MN, *et al.* 2019. Cryptic phenology in plants: Case studies, implications, and recommendations. *Glob Chang Biol* **25**: 3591–608.

Aleixo I, Norris D, Hemerik L, *et al.* 2019. Amazonian rainforest tree mortality driven by climate and functional traits. *Nat Clim Chang* **9**: 384–8.

Alencar AAC, Solórzano LA, and Nepstad DC. 2004. Modeling Forest understory fires in an eastern Amazonian landscape. *Ecol Appl* **14**: 139–49.

Allen GH and Pavelsky TM. 2018. Global extent of rivers and streams. *Science* **361**: 585–8.

Almeida RM, Shi Q, Gomes-Selman JM, *et al.* 2019. Reducing greenhouse gas emissions of Amazon hydropower with strategic dam planning. *Nat Commun* **10**: 4281.

Amaral JHF, Farjalla VF, Melack JM, *et al.* 2019. Seasonal and spatial variability of CO 2 in aquatic environments of the central lowland Amazon basin. *Biogeochemistry* **143**: 133–49.

Amaral JHF, Melack JM, Barbosa PM, *et al.* 2020. Carbon dioxide fluxes to the atmosphere from waters within flooded forests in the Amazon basin. *J Geophys Res Biogeosciences* **125**: e2019JG005293.

Amaral JHF, Suhett AL, Melo S, and Farjalla VF. 2013. Seasonal variation and interaction of photodegradation and microbial metabolism of DOC in black water Amazonian ecosystems. *Aquat Microb Ecol* **70**: 157–68.

Amaral JHF. 2017. Dinâmica do CO_2 em ecossistemas aquáticos na bacia Central Amazônica: uma abordagem em múltiplas escalas. *Dissertation*. Instituto Nacional de Pesquisas da Amazônia, Manaus

Ancellet G, Beekmann M, and Papayannis A. 1994. Impact of a cut-off low development on downward transport of ozone in the troposphere. *J Geophys Res Atmos* **99**: 3451–68.

Anderegg WRL, Konings AG, Trugman AT, *et al.* 2018. Hydraulic diversity of forests regulates ecosystem resilience during drought. *Nature* **561**: 538–41.

Anderson LO, Malhi Y, Aragão LEOC, *et al.* 2010. Remote sensing detection of droughts in Amazonian forest canopies. *New Phytol* **187**: 733–50.

Andreae MO and Rosenfeld D. 2008. Aerosol-cloud-precipitation interactions. Part 1. The nature and sources of cloud-active aerosols. *Earth-Science Rev* **89**: 13–41.

Andreae MO, Acevedo OC, Araùjo A, *et al.* 2015. The Amazon Tall Tower Observatory (ATTO): overview of pilot measurements on ecosystem ecology, meteorology, trace gases, and aerosols. *Atmos Chem Phys* **15**: 10723–76.

Andreae MO, Afchine A, Albrecht R, *et al.* 2018. Aerosol characteristics and particle production in the upper troposphere over the Amazon Basin. *Atmos Chem Phys* **18**: 921–61.

Andreae MO. 2007. Atmosphere. Aerosols before pollution. *Science* **315**: 50–1.

Andreae MO. 2019. Emission of trace gases and aerosols from biomass burning--an updated assessment. *Atmos Chem Phys* **19**: 8523–46.

Aragão LEOC, Anderson LO, Fonseca MG, *et al.* 2018. 21st Century drought-related fires counteract the decline of Amazon deforestation carbon emissions. *Nat Commun* **9**: 536.

Aragão LEOC, Malhi Y, Barbier N, *et al.* 2008. Interactions between rainfall, deforestation and fires during recent years in the Brazilian Amazonia. *Philos Trans R Soc B Biol Sci* **363**: 1779–85.

Aragão LEOC, Malhi Y, Roman-Cuesta RM, *et al.* 2007. Spatial patterns and fire response of recent Amazonian droughts. *Geophys*

Res Lett **34**: L07701.

Aragão LEOC, Poulter B, Barlow JB, *et al.* 2014. Environmental change and the carbon balance of Amazonian forests. *Biol Rev* **89**: 913–31.

Aragão LEOC, Malhi Y, Metcalfe DB, et al. 2009. Above- and below-ground net primary productivity across ten Amazonian forests on contrasting soils. Biogeosciences **6**: 2759–78.

Araujo RF, Nelson BW, Celes CHS, and Chambers JQ. 2017. Regional distribution of large blowdown patches across Amazonia in 2005 caused by a single convective squall line. *Geophys Res Lett* **44**: 7793–8.

Artaxo P, Hansson H-C, and Andreae, MO. Tropical and Boreal Forests - Atmosphere interactions. *Submitt to Tellus.*

Baars H, Ansmann A, Althausen D, *et al.* 2011. Further evidence for significant smoke transport from Africa to Amazonia. *Geophys Res Lett* **38**.

Baker IT, Prihodko L, Denning AS, *et al.* 2008. Seasonal drought stress in the Amazon: Reconciling models and observations. *J Geophys Res Biogeosciences* **113**.

Barbosa PM, Melack JM, Amaral JHF, *et al.* 2020. Dissolved methane concentrations and fluxes to the atmosphere from a tropical floodplain lake. *Biogeochemistry* **148**: 129–51.

Barbosa PM, Melack JM, Amaral JHF, *et al.* 2021. Large Seasonal and Habitat Differences in Methane Ebullition on the Amazon Floodplain. *J Geophys Res Biogeosciences* **126**.

Barbosa PM, Melack JM, Farjalla VF, *et al.* 2016. Diffusive methane fluxes from Negro, Solimões and Madeira rivers and fringing lakes in the Amazon basin. *Limnol Oceanogr* **61**: S221--S237.

Barichivich J, Gloor E, Peylin P, *et al.* 2018. Recent intensification of Amazon flooding extremes driven by strengthened Walker circulation. *Sci Adv* **4**: eaat8785.

Barros F de V, Bittencourt PRL, Brum M, *et al.* 2019. Hydraulic traits explain differential responses of Amazonian forests to the 2015 El Niño-induced drought. *New Phytol* **223**: 1253–66.

Barros N, Cole JJ, Tranvik LJ, *et al.* 2011. Carbon emission from hydroelectric reservoirs linked to reservoir age and latitude. *Nat Geosci* **4**: 593–6.

Basso LS, Gatti L V, Gloor M, *et al.* 2016. Seasonality and interannual variability of CH4 fluxes from the eastern Amazon Basin inferred from atmospheric mole fraction profiles. *J Geophys Res Atmos* **121**: 168–84.

Beer C, Reichstein M, Tomelleri E, *et al.* 2010. Terrestrial Gross Carbon Dioxide Uptake: Global Distribution and Covariation with Climate. *Science* **329**: 834–8.

Beighley RE and Gummadi V. 2011. Developing channel and floodplain dimensions with limited data: a case study in the Amazon Basin. *Earth Surf Process Landforms* **36**: 1059–71.

Belger L, Forsberg BR, and Melack JM. 2011. Carbon dioxide and methane emissions from interfluvial wetlands in the upper Negro River basin, Brazil. *Biogeochemistry* **105**: 171–83.

Bergamaschi P, Frankenberg C, Meirink JF, *et al.* 2009. Inverse modeling of global and regional CH4 emissions using SCIAMACHY satellite retrievals. *J Geophys Res Atmos* **114**.

Bessagnet B, Menut L, Curci G, *et al.* 2008. Regional modeling of carbonaceous aerosols over Europe—focus on secondary organic aerosols. *J Atmos Chem* **61**: 175–202.

Bloom AA, Lee-Taylor J, Madronich S, *et al.* 2010. Global methane emission estimates from ultraviolet irradiation of terrestrial plant foliage. *New Phytol* **187**: 417–25.

Bracho-Nunez A, Knothe NM, Costa WR, *et al.* 2012. Root anoxia effects on physiology and emissions of volatile organic compounds (VOC) under short-and long-term inundation of trees from Amazonian floodplains. *Springerplus* **1**: 1–16.

Brando PM, Goetz SJ, Baccini A, *et al.* 2010. Seasonal and interannual variability of climate and vegetation indices across the Amazon. *Proc Natl Acad Sci* **107**: 14685–90.

Breuer L, Papen H, and Butterbach-Bahl K. 2000. N2O emission from tropical forest soils of Australia. *J Geophys Res Atmos* **105**: 26353–67.

Brienen RJW, Phillips OL, Feldpausch TR, *et al.* 2015. Long-term decline of the Amazon carbon sink. *Nature* **519**: 344–8.

Brum M, Vadeboncoeur MA, Ivanov V, *et al.* 2019. Hydrological niche segregation defines forest structure and drought tolerance strategies in a seasonal Amazon forest. *J Ecol* **107**: 318–33.

Buendía C, Kleidon A, Manzoni S, *et al.* 2018. Evaluating the effect of nutrient redistribution by animals on the phosphorus cycle of lowland Amazonia. *Biogeosciences* **15**: 279–95.

Buscardo E, Nardoto G, Luizão F, *et al.* 2016. The Biogeochemistry of the Main Forest Vegetation Types in Amazonia. In: Interactions between biosphere, atmosphere and human land use in the Amazon basin. Springer.

Bush MB. 2017. The resilience of Amazonian forests. *Nature* **541**: 167–8.

Bustamante MMC, Keller M, and Silva DA. 2009. Sources and sinks of trace gases in Amazonia and the Cerrado. In: In Amazonia and Global Change. Wiley Blackwell.

Cano-Crespo A, Oliveira PJC, Boit A, et al. 2015. Forest edge burning in the Brazilian Amazon promoted by escaping fires from managed pastures. *J Geophys Res Biogeosciences* **120**: 2095–107.

Cardoso MF, Hurtt GC, Moore B, *et al.* 2003. Projecting future fire activity in Amazonia. *Glob Chang Biol* **9**: 656–69.

Carmo JB do, Keller M, Dias JD, *et al.* 2006. A source of methane from upland forests in the Brazilian Amazon. *Geophys Res Lett* **33**.

Carvalho MR, Jaramillo C, la Parra F de, *et al.* 2021. Extinction at the end-Cretaceous and the origin of modern Neotropical rainforests. *Science* **372**: 63–8.

Castello L, McGrath DG, Hess LL, *et al.* 2013. The vulnerability of Amazon freshwater ecosystems. *Conserv Lett* **6**: 217–29.

Castro AO, Chen J, Zang CS, *et al.* 2020. OCO-2 Solar-Induced Chlorophyll Fluorescence Variability across Ecoregions of the Amazon Basin and the Extreme Drought Effects of El Niño (2015–2016). *Remote Sens* **12**: 1202.

Chambers JQ, Higuchi N, Schimel JP, *et al.* 2000. Decomposition and carbon cycling of dead trees in tropical forests of the central Amazon. *Oecologia* **122**: 380–8.

Chambers JQ, Negron-Juarez RI, Marra DM, et al. 2013. The steady-state mosaic of disturbance and succession across an old-growth central Amazon forest landscape. *Proc Natl Acad Sci U S A* **110**: 3949–54.

Chen Q, Farmer DK, Rizzo L V, *et al.* 2015. Submicron particle mass concentrations and sources in the Amazonian wet season (AMAZE-08). *Atmos Chem Phys* **15**: 3687–701.

Chen Q, Farmer DK, Schneider J, *et al.* 2009. Mass spectral charac-

terization of submicron biogenic organic particles in the Amazon Basin. *Geophys Res Lett* **36**.

Chen Y, Randerson JT, Werf GR Van Der, *et al.* 2010. Nitrogen deposition in tropical forests from savanna and deforestation fires. *Glob Chang Biol* **16**: 2024–38.

China S, Wang B, Weis J, *et al.* 2016. Rupturing of biological spores as a source of secondary particles in Amazonia. *Environ Sci |& Technol* **50**: 12179–86.

Ciais P, Sabine C, Bala G, *et al.* 2014. Carbon and other biogeochemical cycles. In: Climate change 2013: the physical science basis. Contribution of Working Group I to the Fifth Assessment Report of the Intergovernmental Panel on Climate Change. Cambridge University Press.

Cicerone RJ. 1987. Changes in Stratospheric Ozone. *Science* **237**: 35–42.

Clifton OE, Fiore AM, Massman WJ, *et al.* 2020. Dry deposition of ozone over land: processes, measurement, and modeling. *Rev Geophys* **58**: e2019RG000670.

Cochrane MA and Laurance WF. 2002. Fire as a large-scale edge effect in Amazonian forests. *J Trop Ecol*: 311–25.

Cochrane MA and Laurance WF. 2008. Synergisms among fire, land use, and climate change in the Amazon. *Ambio*: 522–7.

Cochrane MA. 2001. Synergistic interactions between habitat fragmentation and fire in evergreen tropical forests. *Conserv Biol* **15**: 1515–21.

Coe MT, Costa MH, and Howard EA. 2008. Simulating the surface waters of the Amazon River basin: impacts of new river geomorphic and flow parameterizations. *Hydrol Process An Int J* **22**: 2542–53.

Conrad R. 2009. The global methane cycle: recent advances in understanding the microbial processes involved. *Environ Microbiol Rep* **1**: 285–92.

Cooper OR, Parrish DD, Ziemke J, *et al.* 2014. Global distribution and trends of tropospheric ozone: An observation-based reviewGlobal distribution and trends of tropospheric ozone. *Elem Sci Anthr* **2**.

Cosme LHM, Schietti J, Costa FRC, and Oliveira RS. 2017. The importance of hydraulic architecture to the distribution patterns of trees in a central Amazonian forest. *New Phytol* **215**: 113–25.

da Costa ACL, Galbraith D, Almeida S, *et al.* 2010. Effect of 7 yr of experimental drought on vegetation dynamics and biomass storage of an eastern Amazonian rainforest. *New Phytol* **187**: 579–91.

Covey KR and Megonigal JP. 2019. Methane production and emissions in trees and forests. *New Phytol* **222**: 35–51.

Covey KR, Mesquita CPB de, Oberle B, *et al.* 2016. Greenhouse trace gases in deadwood. *Biogeochemistry* **130**: 215–26.

Cruvinel ÊBF, Bustamante MMC da, Kozovits AR, and Zepp RG. 2011. Soil emissions of NO, N2O and CO2 from croplands in the savanna region of central Brazil. *Agric Ecosyst Environ* **144**: 29–40.

Cuevas E and Medina E. 1988. Nutrient dynamics within Amazonian forests. *Oecologia* **76**: 222–35.

Dal Maso M, Kulmala M, Riipinen I, *et al.* 2005. Formation and growth of fresh atmospheric aerosols: eight years of aerosol size distribution data from SMEAR II, Hyytiala, Finland. *Boreal Environ Res* **10**: 323.

Davidson EA and Artaxo P. 2004. Globally significant changes in biological processes of the Amazon Basin: results of the Large-scale Biosphere--Atmosphere Experiment. *Glob Chang Biol* **10**: 519–29.

Davidson EA and Kanter D. 2014. Inventories and scenarios of nitrous oxide emissions. *Environ Res Lett* **9**: 105012.

Davidson EA, Bustamante MMC, and Siqueira Pinto A de. 2001. Emissions of Nitrous Oxide and Nitric Oxide from Soils of Native and Exotic Ecosystems of the Amazon and Cerrado Regions of Brazil. *Sci World J* **1**: 312–9.

Davidson EA, Carvalho CJR de, Figueira AM, *et al.* 2007. Recuperation of nitrogen cycling in Amazonian forests following agricultural abandonment. *Nature* **447**: 995–8.

Davidson EA, Ishida FY, and Nepstad DC. 2004. Effects of an experimental drought on soil emissions of carbon dioxide, methane, nitrous oxide, and nitric oxide in a moist tropical forest. *Glob Chang Biol* **10**: 718–30.

Davidson EA, Nepstad DC, Ishida FY, and Brando PM. 2008. Effects of an experimental drought and recovery on soil emissions of carbon dioxide, methane, nitrous oxide, and nitric oxide in a moist tropical forest. *Glob Chang Biol* **14**: 2582–90.

Deemer BR, Harrison JA, Li S, *et al.* 2016. Greenhouse gas emissions from reservoir water surfaces: a new global synthesis. *Bioscience* **66**: 949–64.

Devol AH, Richey JE, and Forsberg BR. 1991. Phosphorus in the Amazon River mainstem: Concentrations, forms, and transport to the ocean. *Phosphorus Cycles Terr Aquat Ecosyst*: 9–23.

Doughty CE, Metcalfe DB, Girardin CAJ, *et al.* 2015. Drought impact on forest carbon dynamics and fluxes in Amazonia. *Nature* **519**: 78–82.

Doughty CE, Wolf A, and Malhi Y. 2013. The legacy of the Pleistocene megafauna extinctions on nutrient availability in Amazonia. *Nat Geosci* **6**: 761–4.

Dutaur L and Verchot L V. 2007. A global inventory of the soil CH_4 sink. *Global Biogeochem Cycles* **21**: 4013.

Ellis EE, Richey JE, Aufdenkampe AK, *et al.* 2012. Factors controlling water-column respiration in rivers of the central and southwestern Amazon Basin. *Limnol Oceanogr* **57**: 527–40.

Espírito-Santo FDB, Gloor M, Keller M, *et al.* 2014. Size and frequency of natural forest disturbances and the Amazon forest carbon balance. *Nat Commun* **5**: 3434.

Esquivel-Muelbert A, Phillips OL, Brienen RJW, *et al.* 2020. Tree mode of death and mortality risk factors across Amazon forests. *Nat Commun* **11**: 5515.

Esteban EJL, Castilho C V, Melgaço KL, and Costa FRC. 2021. The other side of droughts: wet extremes and topography as buffers of negative drought effects in an Amazonian forest. *New Phytol* **229**: 1995–2006.

Eva HD, Huber O., Achard F., *et al.* 2005. A proposal for defining the geographical boundaries of Amazonia [Synthesis of the results from an Expert Consultation Workshop organized by the European Commission in collaboration with the Amazon Cooperation Treaty Organization-JRC Ispra, 7-8 June 2005].

Figueiredo V, Enrich-Prast A, and Rütting T. 2019. Evolution of nitrogen cycling in regrowing Amazonian rainforest. *Sci Rep* **9**: 1–8.

Fiore AM, Jacob DJ, Field BD, *et al.* 2002. Linking ozone pollution and climate change: The case for controlling methane. *Geophys*

Res Lett **29**: 25-1-25–4.

Fleischer K, Rammig A, Kauwe MG De, et al. 2019. Amazon forest response to CO2 fertilization dependent on plant phosphorus acquisition. *Nat Geosci* **12**: 736–41.

Fonseca LDM, Dalagnol R, Malhi Y, *et al.* 2019. Phenology and seasonal ecosystem productivity in an Amazonian floodplain forest. *Remote Sens* **11**: 1530.

Fraser A, Palmer PI, Feng L, *et al.* 2014. Estimating regional fluxes of CO2 and CH 4 using space-borne observations of XCH 4: XCO2. *Atmos Chem Phys* **14**: 12883–95.

Fu R and Li W. 2004. The influence of the land surface on the transition from dry to wet season in Amazonia. *Theor Appl Climatol* **78**: 97–110.

Galford GL, Melillo JM, Kicklighter DW, *et al.* 2010. Greenhouse gas emissions from alternative futures of deforestation and agricultural management in the southern Amazon. *Proc Natl Acad Sci* **107**: 19649–54.

Garcia MN, Ferreira MJ, Ivanov V, *et al.* 2021. Importance of hydraulic strategy trade-offs in structuring response of canopy trees to extreme drought in central Amazon. *Oecologia*: 1–12.

Gatti L V., Gloor M, Miller JB, *et al.* 2014. Drought sensitivity of Amazonian carbon balance revealed by atmospheric measurements. *Nature* **506**: 76–80.

Girardin CAJ, Malhi Y, Doughty CE, *et al.* 2016. Seasonal trends of Amazonian rainforest phenology, net primary productivity, and carbon allocation. *Global Biogeochem Cycles* **30**: 700–15.

Gouveia NA, Gherardi DFMM, and Aragão LEOC. 2019. The role of the Amazon river plume on the intensification of the hydrological cycle. *Geophys Res Lett* **46**: 12221–9.

Graham B, Guyon P, Taylor PE, *et al.* 2003. Organic compounds present in the natural Amazonian aerosol: Characterization by gas chromatography--mass spectrometry. *J Geophys Res Atmos* **108**.

Guan K, Pan M, Li H, *et al.* 2015. Photosynthetic seasonality of global tropical forests constrained by hydroclimate. *Nat Geosci* **8**: 284–9.

Guilhen J, Bitar A Al, Sauvage S, *et al.* 2020. Denitrification and associated nitrous oxide and carbon dioxide emissions from the Amazonian wetlands. *Biogeosciences* **17**: 4297–311.

Gut A, Dijk SM Van, Scheibe M, *et al.* 2002a. NO emission from an Amazonian rain forest soil: Continuous measurements of NO flux and soil concentration. *J Geophys Res Atmos* **107**: LBA24.

Gut A, Scheibe M, Rottenberger S, *et al.* 2002b. Exchange fluxes of NO2 and O3 at soil and leaf surfaces in an Amazonian rain forest. *J Geophys Res Atmos* **107**: 8060.

Haffer J. 1969. Speciation in amazonian forest birds. *Science* **165**: 131–7.

Hamilton SK, Sippel SJ, and Melack JM. 1995. Oxygen depletion and carbon dioxide and methane production in waters of the Pantanal wetland of Brazil. *Biogeochemistry* **30**: 115–41.

Hamilton SK, Sippel SJ, and Melack JM. 2002. Comparison of inundation patterns among major South American floodplains. *J Geophys Res Atmos* **107**: LBA--5.

Hasler N and Avissar R. 2007. What controls evapotranspiration in the Amazon basin? *J Hydrometeorol* **8**: 380–95.

Hess LL, Melack JM, Affonso AG, *et al.* 2015. Wetlands of the lowland Amazon basin: Extent, vegetative cover, and dual-season

inundated area as mapped with JERS-1 synthetic aperture radar. *Wetlands* **35**: 745–56.

Hess LL, Melack JM, Novo EMLM, *et al.* 2003. Dual-season mapping of wetland inundation and vegetation for the central Amazon basin. *Remote Sens Environ* **87**: 404–28.

Hu X-M, Fuentes JD, and Zhang F. 2010. Downward transport and modification of tropospheric ozone through moist convection. *J Atmos Chem* **65**: 13–35.

Huete AR, Didan K, Shimabukuro YE, et al. 2006. Amazon rainforests green-up with sunlight in dry season. *Geophys Res Lett* **33**: 6405.

Hubau W, Lewis SL, Phillips OL, et al. 2020. Asynchronous carbon sink saturation in African and Amazonian tropical forests. *Nat* 579: 80–7.

Huffman J, Sinha B, and Garland R. 2012. Zotino Tall Tower Observatory (ZOTTO) View project Seasonal variation in Primary Marine Aerosol source due to Physical and Bio/Chemical processes View project Atmospheric Chemistry and Physics Size distributions and temporal variations of biological aer. *Atmos Chem Phys* **12**: 11997–2019.

Ivanov VY, Hutyra LR, Wofsy SC, *et al.* 2012. Root niche separation can explain avoidance of seasonal drought stress and vulnerability of overstory trees to extended drought in a mature Amazonian forest. *Water Resour Res* **48**: 12507.

Jankowski K, Neill C, Davidson EA, *et al.* 2018. Deep soils modify environmental consequences of increased nitrogen fertilizer use in intensifying Amazon agriculture. *Sci Rep* **8**: 1–11.

Janssen T, Velde Y van der, Hofhansl F, *et al.* 2021. Drought effects on leaf fall, leaf flushing and stem growth in Neotropical forest; reconciling remote sensing data and field observations. *Biogeosciences Discuss*: 1–41.

Jati SR and others. 2013. Emissao de CO2 e CH4 nas savanas úmidas de Roraima.

Johnson CM, Vieira ICG, Zarin DJ, *et al.* 2001. Carbon and nutrient storage in primary and secondary forests in eastern Amazônia. *For Ecol Manage* **147**: 245–52.

Johnson MO, Galbraith D, Gloor M, *et al.* 2016. Variation in stem mortality rates determines patterns of above-ground biomass in Amazonian forests: implications for dynamic global vegetation models. *Glob Chang Biol* **22**: 3996–4013.

Johnson MS, Lehmann J, Riha SJ, *et al.* 2008. CO2 efflux from Amazonian headwater streams represents a significant fate for deep soil respiration. *Geophys Res Lett* **35**.

Jones MO, Kimball JS, and Nemani RR. 2014. Asynchronous Amazon forest canopy phenology indicates adaptation to both water and light availability. *Environ Res Lett* **9**: 124021.

Junk WJ, Piedade MTF, Schöngart J, *et al.* 2011. A classification of major naturally-occurring Amazonian lowland wetlands. *Wetlands* **31**: 623–40.

Keller M, Alencar A, Asner GP, *et al.* 2004. Ecological research in the large-scale biosphere--atmosphere experiment in Amazonia: early results. *Ecol Appl* **14**: 3–16.

Kemenes A, Forsberg BR, and Melack JM. 2007. Methane release below a tropical hydroelectric dam. *Geophys Res Lett* **34**.

Kemenes A, Forsberg BR, and Melack JM. 2011. CO2 emissions from a tropical hydroelectric reservoir (Balbina, Brazil). *J Geophys Res Biogeosciences* **116**.

Kemenes A, Forsberg BR, and Melack JM. 2016. Downstream

emissions of CH_4 and CO_2 from hydroelectric reservoirs (Tucuruí, Samuel, and Curuá-Una) in the Amazon basin. *Inl Waters* **6**: 295–302.

Kesselmeier J and Staudt M. 1999. Biogenic volatile organic compounds (VOC): an overview on emission, physiology and ecology. *J Atmos Chem* **33**: 23–88.

Kesselmeier J, Ciccioli P, Kuhn U, *et al.* 2002. Volatile organic compound emissions in relation to plant carbon fixation and the terrestrial carbon budget. *Global Biogeochem Cycles* **16**: 71–3.

Lähteenoja O, Flores B, and Nelson B. 2013. Tropical peat accumulation in Central Amazonia. *Wetlands* **33**: 495–503.

Lähteenoja O, Reátegui YR, Räsänen M, *et al.* 2012. The large Amazonian peatland carbon sink in the subsiding Pastaza-Marañón foreland basin, P eru. *Glob Chang Biol* **18**: 164–78.

Laothawornkitkul J, Taylor JE, Paul ND, and Hewitt CN. 2009. Biogenic volatile organic compounds in the Earth system. *New Phytol* **183**: 27–51.

Lee J-E, Oliveira RS, Dawson TE, and Fung I. 2005. Root functioning modifies seasonal climate. *Proc Natl Acad Sci* **102**: 17576–81.

Lenhart K, Weber B, Elbert W, *et al.* 2015. Nitrous oxide and methane emissions from cryptogamic covers. *Glob Chang Biol* **21**: 3889–900.

Lent J van, Hergoualch K, and Verchot L V. 2015. Reviews and syntheses: Soil N 2 O and NO emissions from land use and land-use change in the tropics and subtropics: a meta-analysis. *Biogeosciences* **12**: 7299–313.

Less DFS, Cunha AC, Sawakuchi HO, *et al.* 2018. The role of hydrodynamic and biogeochemistry on CO 2 flux and pCO 2 at the Amazon River mouth. *Biogeosciences Discuss*: 1–26.

Levine NM, Zhang K, Longo M, *et al.* 2016. Ecosystem heterogeneity determines the ecological resilience of the Amazon to climate change. *Proc Natl Acad Sci* **113**: 793–7.

Lim YB, Tan Y, Perri MJ, *et al.* 2010. Aqueous chemistry and its role in secondary organic aerosol (SOA) formation. *Atmos Chem Phys* **10**: 10521–39.

Liu Y, Seco R, Kim S, et al. 2018. Isoprene photo-oxidation products quantify the effect of pollution on hydroxyl radicals over Amazonia. *Sci Adv* **4**: eaar2547

Liu Y, Brito J, Dorris MR, *et al.* 2016. Isoprene photochemistry over the Amazon rainforest. *Proc Natl Acad Sci* **113**: 6125–30.

Longo M, Knox RG, Levine NM, *et al.* 2018. Ecosystem heterogeneity and diversity mitigate Amazon forest resilience to frequent extreme droughts. *New Phytol* **219**: 914–31.

Lopes AP, Nelson BW, Wu J, *et al.* 2016. Leaf flush drives dry season green-up of the Central Amazon. *Remote Sens Environ* **182**: 90–8.

Lu X, Zhang L, and Shen L. 2019. Meteorology and climate influences on tropospheric ozone: a review of natural sources, chemistry, and transport patterns. *Curr Pollut Reports* **5**: 238–60.

Macedo MN, Coe MT, DeFries R, *et al.* 2013. Land-use-driven stream warming in southeastern Amazonia. *Philos Trans R Soc B Biol Sci* **368**: 20120153.

Machacova K, Borak L, Agyei T, *et al.* 2021. Trees as net sinks for methane (CH_4) and nitrous oxide (N_2O) in the lowland tropical rain forest on volcanic Réunion Island. *New Phytol* **229**: 1983–94.

Mahowald NM, Artaxo P, Baker AR, *et al.* 2005. Impacts of biomass burning emissions and land use change on Amazonian atmospheric phosphorus cycling and deposition. *Global Biogeochem Cycles* **19**.

Malhi Y, Aragao LEOC, Metcalfe DB, *et al.* 2009a. Comprehensive assessment of carbon productivity, allocation and storage in three Amazonian forests. *Glob Chang Biol* **15**: 1255–74.

Malhi Y, Saatchi S, Girardin C, and Aragão LEOC. 2009b. The production, storage, and flow of carbon in Amazonian forests. In: Amazonia and Global Change. Wiley Blackwell.

Malhi Y, Baker TR, Phillips OL, *et al.* 2004. The above-ground coarse wood productivity of 104 Neotropical forest plots. *Glob Chang Biol* **10**: 563–91.

Malhi Y, Doughty CE, Goldsmith GR, *et al.* 2015. The linkages between photosynthesis, productivity, growth and biomass in lowland Amazonian forests. *Glob Chang Biol* **21**: 2283–95.

Malhi Y, Girardin CAJ, Goldsmith GR, *et al.* 2017. The variation of productivity and its allocation along a tropical elevation gradient: a whole carbon budget perspective. *New Phytol* **214**: 1019–32.

Markewitz D, Davidson E, Moutinho P, and Nepstad D. 2004. Nutrient loss and redistribution after forest clearing on a highly weathered soil in Amazonia. *Ecol Appl* **14**: 177–99.

Martin ST, Andreae MO, Artaxo P, *et al.* 2010. Sources and properties of Amazonian aerosol particles. *Rev Geophys* **48**.

Martinelli LA, Pinto A de S, Nardoto GB, *et al.* 2012. Nitrogen mass balance in the Brazilian Amazon: an update. *Brazilian J Biol* **72**: 683–90.

Martinson GO, Werner FA, Scherber C, *et al.* 2010. Methane emissions from tank bromeliads in neotropical forests. *Nat Geosci* **3**: 766–9.

Martius C, Waßmann R, Thein U, *et al.* 1993. Methane emission from wood-feeding termites in Amazonia. *Chemosphere* **26**: 623–32.

Maslin M, Malhi Y, Phillips O, and Cowling S. 2005. New views on an old forest: Assessing the longevity, resilience and future of the Amazon rainforest. *Trans Inst Br Geogr* **30**: 477–99.

Matson PA and Vitousek PM. 1990. Ecosystem approach to a global nitrous oxide budget. *Bioscience* **40**: 667–72.

Mayle FE, Beerling DJ, Gosling WD, and Bush MB. 2004. Responses of Amazonian ecosystems to climatic and atmospheric carbon dioxide changes since the last glacial maximum. In: Philosophical Transactions of the Royal Society B: Biological Sciences. Royal Society.

Mayorga E, Aufdenkampe AK, Masiello CA, *et al.* 2005. Young organic matter as a source of carbon dioxide outgassing from Amazonian rivers. *Nature* **436**: 538–41.

Melack JM and Hess LL. 2010. Remote Sensing of the Distribution and Extent of Wetlands in the Amazon Basin. In: Junk W., Piedade M., Wittmann F., Schöngart J., Parolin P. (eds) *Amazonian Floodplain Forests. Ecological Studies* (Analysis and Synthesis), vol **210**. Springer, Dordrecht. https://doi.org/10.1007/978-90-481-8725-6_3.

Melack JM and Engle DL. 2009. An organic carbon budget for an Amazon floodplain lake. *Int Vereinigung für Theor und Angew Limnol Verhandlungen* **30**: 1179–82.

Melack JM, Hess LL, Gastil M, *et al.* 2004. Regionalization of methane emissions in the Amazon Basin with microwave remote

sensing. *Glob Chang Biol* **10**: 530–44.

Melack JM, Novo E, Forsberg BR, *et al.* 2009. Floodplain ecosystem processes. *Amaz Glob Chang* **186**: 525–41.

Melack JM. 2016. Aquatic ecosystems. In: Nagy L, Forsberg B, Artaxo P (Eds). Interactions between biosphere, atmosphere and human land use in the Amazon Basin. *Ecological Studies* **227**. Springer.

Melillo JM, Steudler PA, Feigl BJ, *et al.* 2001. Nitrous oxide emissions from forests and pastures of various ages in the Brazilian Amazon. *J Geophys Res Atmos* **106**: 34179–88.

Metcalfe DB, Meir P, Aragão LEOC, *et al.* 2008. The effects of water availability on root growth and morphology in an Amazon rainforest. *Plant Soil* **311**: 189–99.

Meurer KHE, Franko U, Stange CF, *et al.* 2016. Direct nitrous oxide (N2O) fluxes from soils under different land use in Brazil—a critical review. *Environ Res Lett* **11**: 23001.

Miller JB, Gatti L V, d'Amelio MTS, *et al.* 2007. Airborne measurements indicate large methane emissions from the eastern Amazon basin. *Geophys Res Lett* **34**.

Moran-Zuloaga D, Ditas F, Walter D, *et al.* 2018. Long-term study on coarse mode aerosols in the Amazon rain forest with the frequent intrusion of Saharan dust plumes. *Atmos Chem Phys* **18**: 10055–88.

Morton DC, Nagol J, Carabajal CC, *et al.* 2014. Amazon forests maintain consistent canopy structure and greenness during the dry season. *Nature* **506**: 221–4.

Nardoto GB, Quesada CA, Patiño S, *et al.* 2014. Basin-wide variations in Amazon forest nitrogen-cycling characteristics as inferred from plant and soil 15 N: 14 N measurements. *Plant Ecol Divers* **7**: 173–87.

Nelson BW, Kapos V, Adams JB, *et al.* 1994. Forest disturbance by large blowdowns in the Brazilian Amazon. *Ecology* **75**: 853–8.

Nepstad D, Lefebvre P, Silva U da, *et al.* 2004. Amazon drought and its implications for forest flammability and tree growth: A basin-wide analysis. *Glob Chang Biol* **10**: 704–17.

Nepstad DC, Carvalho CR De, Davidson EA, *et al.* 1994. The role of deep roots in the hydrological and carbon cycles of Amazonian forests and pastures. *Nature* **372**: 666–9.

Nölscher AC, Yáñez-Serrano AM, Wolff S, *et al.* 2016. Unexpected seasonality in quantity and composition of Amazon rainforest air reactivity. *Nat Commun* **7**: 1–12.

Oliveira Marques JD, Luizão FJ, Teixeira WG, *et al.* 2017. Soil Carbon Stocks under Amazonian Forest: Distribution in the Soil Fractions and Vulnerability to Emission. *Open J For* **07**: 121–42.

Oliveira RS, Costa FRC, Baalen E van, *et al.* 2019. Embolism resistance drives the distribution of Amazonian rainforest tree species along hydro-topographic gradients. *New Phytol* **221**: 1457–65.

Oliveira RS, Dawson TE, Burgess SSO, and Nepstad DC. 2005. Hydraulic redistribution in three Amazonian trees. *Oecologia* **145**: 354–63.

Osborne CP. 2008. Atmosphere, ecology and evolution: What drove the Miocene expansion of C4 grasslands? *J Ecol* **96**: 35–45.

Pacheco FS, Ometto J, Gomes L, *et al.* Nutrient balance and use efficiency in agricultural lands in the Vermelho River watershed, Upper Pantanal, Brazil. *J Geophys Res Biogeosciences*: e2020JG005673.

Pacifico F, Folberth GA, Sitch S, *et al.* 2015. Biomass burning related ozone damage on vegetation over the Amazon forest: a model sensitivity study. *Atmos Chem Phys* **15**: 2791–804.

Paiva RCD, Buarque DC, Collischonn W, *et al.* 2013. Large-scale hydrologic and hydrodynamic modeling of the Amazon River basin. *Water Resour Res* **49**: 1226–43.

Pangala SR, Enrich-Prast A, Basso LS, *et al.* 2017. Large emissions from floodplain trees close the Amazon methane budget. *Nature* **552**: 230–4.

Parrens M, Bitar A Al, Frappart F, *et al.* 2019. High resolution mapping of inundation area in the Amazon basin from a combination of L-band passive microwave, optical and radar datasets. *Int J Appl Earth Obs Geoinf* **81**: 58–71.

Peñuelas J and Staudt M. 2010. BVOCs and global change. *Trends Plant Sci* **15**: 133–44.

Pfannerstill EY, Nölscher AC, Yáñez-Serrano AM, *et al.* 2018. Total OH reactivity changes over the Amazon rainforest during an El Niño event. *Front For Glob Chang* **1**: 12.

Phillips OL, Aragão LEOCOC, Lewis SL, *et al.* 2009. Drought sensitivity of the Amazon rainforest. *Science* **323**: 1344–7.

Phillips OL, Heijden G Van Der, Lewis SL, *et al.* 2010. Drought-mortality relationships for tropical forests. *New Phytol* **187**: 631–46.

Pöhlker C, Walter D, Paulsen H, *et al.* 2019. Land cover and its transformation in the backward trajectory footprint region of the Amazon Tall Tower Observatory. *Atmos Chem Phys* **19**: 8425–70.

Pöhlker C, Wiedemann KT, Sinha B, *et al.* 2012. Biogenic potassium salt particles as seeds for secondary organic aerosol in the Amazon. *Science* **337**: 1075–8.

Pöhlker ML, Ditas F, Saturno J, *et al.* 2018. Long-term observations of cloud condensation nuclei over the Amazon rain forest-Part 2: Variability and characteristics of biomass burning, long-range transport, and pristine rain forest aerosols. *Atmos Chem Phys* **18**: 10289–331.

Pöhlker ML, Pöhlker C, Klimach T, *et al.* 2016. Long-term observations of atmospheric aerosol, cloud condensation nuclei concentration and hygroscopicity in the Amazon rain forest-Part 1: Size-resolved characterization and new model parameterizations for CCN prediction. *Atmos Chem Phys Discuss*.

Pöschl U, Martin ST, Sinha B, *et al.* 2010. Rainforest aerosols as biogenic nuclei of clouds and precipitation in the Amazon. *Science* **329**: 1513–6.

Poulter B, Aragão L, Heyder U, et al. 2010. Net biome production of the Amazon Basin in the 21st century. *Glob Chang Biol* **16**: 2062–75.

Prenni AJ, Petters MD, Kreidenweis SM, *et al.* 2009. Relative roles of biogenic emissions and Saharan dust as ice nuclei in the Amazon basin. *Nat Geosci* **2**: 402–5.

Prigent C, Jimenez C, and Bousquet P. 2020. Satellite-Derived Global Surface Water Extent and Dynamics Over the Last 25 Years (GIEMS-2). *J Geophys Res Atmos* **125**: e2019JD030711.

Qie L, Lewis SL, Sullivan MJP, *et al.* 2017. Long-term carbon sink in Borneo's forests halted by drought and vulnerable to edge effects. *Nat Commun* **8**: 1–11.

Quesada CA, Lloyd J, Schwarz M, *et al.* 2010. Variations in chemical and physical properties of Amazon forest soils in relation to their genesis. *Biogeosciences* **7**: 1515–41.

Quesada CA, Paz C, Oblitas Mendoza E, *et al.* 2020. Variations in

soil chemical and physical properties explain basin-wide Amazon forest soil carbon concentrations. *Soil* **6**: 53–88.

Quesada CA, Phillips OL, Schwarz M, *et al.* 2012. Basin-wide variations in Amazon forest structure and function are mediated by both soils and climate. *Biogeosciences* **9**: 2203–46.

Raich JW. 2017. Temporal variability of soil respiration in experimental tree plantations in lowland Costa Rica. *Forests* **8**: 40.

Rasera M de FFL, Ballester MVR, Krusche A V, *et al.* 2008. Estimating the Surface Area of Small Rivers in the Southwestern Amazon and Their Role in CO2 Outgassing. *Earth Interact* **12**: 1–16.

Ratana P, Huete A, and Didan K. 2006. MODIS EVIbased Variability in Amazon Phenology across the Rainforest-Cerrado Ecotone. In: 2006 IEEE International Symposium on Geoscience and Remote Sensing: 1942-1944.

Ratana P, Huete AR, Restrepo-Coupe N, and Shimabukuro YE. 2012. MODIS EVI Landscape Phenology across Amazon Rainforest-Cerrado Ecotone. In: AGU Fall Meeting Abstracts.

Ray D, Nepstad D, and Moutinho P. 2005. Micrometeorological and canopy controls of fire susceptibility in a forested Amazon landscape. *Ecol Appl* **15**: 1664–78.

Reich PB, Uhl C, Walters MB, *et al.* 2004. Leaf demography and phenology in Amazonian rain forest: a census of 40 000 leaves of 23 tree species. *Ecol Monogr* **74**: 3–23.

Reis CRG, Pacheco FS, Reed SC, *et al.* 2020. Biological nitrogen fixation across major biomes in Latin America: Patterns and global change effects. *Sci Total Environ* **746**: 140998.

Remington S, Krusche A, and Richey J. 2011. Effects of DOM photochemistry on bacterial metabolism and CO 2 evasion during falling water in a humic and a whitewater river in the Brazilian Amazon. *Biogeochemistry* **105**: 185–200.

Resende AF, Piedade MTF, Feitosa YO, *et al.* 2020. Flood-pulse disturbances as a threat for long-living Amazonian trees. *New Phytol* **227**: 1790–803.

Restrepo-Coupe N, Levine NM, Christoffersen BO, *et al.* 2017. Do dynamic global vegetation models capture the seasonality of carbon fluxes in the Amazon basin? A data-model intercomparison. *Glob Chang Biol* **23**: 191–208.

Restrepo-Coupe N, Rocha HR da, Hutyra LR, *et al.* 2013. What drives the seasonality of photosynthesis across the Amazon basin? A cross-site analysis of eddy flux tower measurements from the Brasil flux network. *Agric For Meteorol* **182**: 128–44.

Richey JE, Hedges JI, Devol AH, *et al.* 1990. Biogeochemistry of carbon in the Amazon River. *Limnol Oceanogr* **35**: 352–71.

Richey JE, Krusche A V, Johnson MS, *et al.* 2009. The role of rivers in the regional carbon balance. In: Gash J, Keller M, Bustamante M, Dias P (Eds). Amazonia and Global Change. Geophysical Mono-graph.

Richey JE, Melack JM, Aufdenkampe AK, *et al.* 2002. Outgassing from Amazonian rivers and wetlands as a large tropical source of atmospheric CO2. *Nature* **416**: 617–20.

Rizzo LV, Roldin P, Brito J, *et al.* 2018. Multi-year statistical and modeling analysis of submicrometer aerosol number size distributions at a rain forest site in Amazonia. *Atmos Chem Phys* **18**: 10255–74.

Rizzolo JA, Barbosa CGG, Borillo GC, *et al.* 2017. Soluble iron nutrients in Saharan dust over the central Amazon rainforest. *Atmos Chem Phys* **17**: 2673–87.

Rosenqvist Å, Forsberg BR, Pimentel T, *et al.* 2002. The use of spaceborne radar data to model inundation patterns and trace gas emissions in the central Amazon floodplain. *Int J Remote Sens* **23**: 1303–28.

Rowland L, Costa ACL da, Galbraith DR, *et al.* 2015. Death from drought in tropical forests is triggered by hydraulics not carbon starvation. *Nature* **528**: 119–22.

Rudorff CM, Melack JM, MacIntyre S, *et al.* 2011. Seasonal and spatial variability of CO 2 emission from a large floodplain lake in the lower Amazon. *J Geophys Res* **116**: G04007.

Rummel U, Ammann C, Kirkman GA, *et al.* 2007. Seasonal variation of ozone deposition to a tropical rain forest in southwest Amazonia. *Atmos Chem Phys* **7**: 5415–35.

Saatchi SS, Houghton RA, Alvalá RCDS, et al. 2007. Distribution of aboveground live biomass in the Amazon basin. *Glob Chang Biol* **13**: 816–37.

Saito M, Kim H-SS, Ito A, *et al.* 2016. Enhanced methane emissions during Amazonian drought by biomass burning. *PLoS One* **11**: e0166039.

Salazar D, Lokvam J, Mesones I, *et al.* 2018. Origin and maintenance of chemical diversity in a species-rich tropical tree lineage. *Nat Ecol Evol* **2**: 983–90.

Saleska SR, Didan K, Huete AR, and Rocha HR Da. 2007. Amazon forests green-up during 2005 drought. *Science* **318**: 612.

Saleska SR, Miller SD, Matross DM, *et al.* 2003. Carbon in Amazon forests: unexpected seasonal fluxes and disturbance-induced losses. *Science* **302**: 1554–7.

Saleska SR, Wu J, Guan K, *et al.* 2016. Dry-season greening of Amazon forests. *Nature* **531**: E4--E5.

Samanta A, Ganguly S, Hashimoto H, *et al.* 2010. Amazon forests did not green-up during the 2005 drought. *Geophys Res Lett* **37**.

Santos VAHF dos, Ferreira MJ, Rodrigues JVFC, *et al.* 2018. Causes of reduced leaf-level photosynthesis during strong El Niño drought in a Central Amazon forest. *Glob Chang Biol* **24**: 4266–79.

Saturno J, Holanda BA, Pöhlker C, *et al.* 2018. Black and brown carbon over central Amazonia: long-term aerosol measurements at the ATTO site. *Atmos Chem Phys* **18**: 12817–43.

Saunois M, R. Stavert A, Poulter B, *et al.* 2020. The global methane budget 2000-2017. *Earth Syst Sci Data* **12**: 1561–623.

Sawakuchi HO, Bastviken D, Sawakuchi AO, *et al.* 2014. Methane emissions from Amazonian Rivers and their contribution to the global methane budget. *Glob Chang Biol* **20**: 2829–40.

Sawakuchi HO, Neu V, Ward ND, *et al.* 2017. Carbon dioxide emissions along the lower Amazon River. *Front Mar Sci* **4**: 76.

Schöngart J and Wittmann F. 2010. Biomass and net primary production of central Amazonian floodplain forests. In: Junk W, Piedade M, Wittmann F, *et al.* (Eds). Amazonian Floodplain Forests. Springer.

Shuttleworth WJ. 1988. Evaporation from Amazonian rainforest. *Proc R Soc London Ser B Biol Sci* **233**: 321–46.

Silva CVJ, Aragão LEOC, Young PJ, *et al.* 2020. Estimating the multi-decadal carbon deficit of burned Amazonian forests. *Environ Res Lett* **15**: 114023.

Sippel SJ, Hamilton SK, and Melack JM. 1992. Inundation area and morphometry of lakes on the Amazon River floodplain, Brazil. *Arch für Hydrobiol* **123**: 385–400.

Sismanoglu RA and Setzer AW. 2005. Risco de fogo da vegetaçao na América do Sul: comparaçao de três versoes na estiagem de

2004. *XII Simpósio Bras Sensoriamento Remoto, Goiania, Brazil*: 16–21.

Smith MN, Taylor TC, Haren J van, *et al.* 2020. Empirical evidence for resilience of tropical forest photosynthesis in a warmer world. *Nat Plants* **6**: 1225–30.

Sousa TR, Schietti J, Souza F de, *et al.* 2020. Palms and trees resist extreme drought in Amazon forests with shallow water tables. *J Ecol* **108**: 2070–82.

Stanley EH, Casson NJ, Christel ST, *et al.* 2016. The ecology of methane in streams and rivers: patterns, controls, and global significance. *Ecol Monogr* **86**: 146–71.

Surratt JD, Chan AWH, Eddingsaas NC, *et al.* 2010. Reactive intermediates revealed in secondary organic aerosol formation from isoprene. *Proc Natl Acad Sci* **107**: 6640–5.

Syakila A and Kroeze C. 2011. The global nitrous oxide budget revisited. *Greenh gas Meas Manag* **1**: 17–26.

Teh YA, Silver WL, and Conrad ME. 2005. Oxygen effects on methane production and oxidation in humid tropical forest soils. *Glob Chang Biol* **11**: 1283–97.

Tian H, Melillo JM, Kicklighter DW, *et al.* 1998. Effect of interannual climate variability on carbon storage in Amazonian ecosystems. *Nature* **396**: 664–7.

Tian H, Xu R, Canadell JG, *et al.* 2020. A comprehensive quantification of global nitrous oxide sources and sinks. *Nature* **586**: 248–56.

Tian H, Yang J, Lu C, *et al.* 2018. The global N2O model intercomparison project. *Bull Am Meteorol Soc* **99**: 1231–51.

Townsend AR, Cleveland CC, Houlton BZ, et al. 2011. Multi-element regulation of the tropical forest carbon cycle. *Front Ecol Environ* **9**: 9–17.

Tunnicliffe RL, Ganesan AL, Parker RJ, *et al.* 2020. Quantifying sources of Brazil's CH4 emissions between 2010 and 2018 from satellite data. *Atmos Chem Phys* **20**: 13041–67.

Van Asperen H, Alves-Oliveira JR, Warneke T, *et al.* 2021. The role of termite CH4 emissions on the ecosystem scale: A case study in the Amazon rainforest. *Biogeosciences* **18**: 2609–25.

van der Molen MK, Dolman AJ, Ciais P, et al. 2011. Drought and ecosystem carbon cycling. *Agric For Meteorol* **151**: 765–73.

Verchot L V., Davidson EA, Cattânio JH, and Ackerman IL. 2000. Land-use change and biogeochemical controls of methane fluxes in soils of eastern Amazonia. *Ecosystems* **3**: 41–56.

Vitoussek PM, Sanford RL, Vitousek PM, and Sanford Jr RL. 1986. Nutrient cycling in moist tropical forest. *Annu Rev Ecol Syst* **17**: 137–67.

Wagner FH, Hérault B, Rossi V, *et al.* 2017. Climate drivers of the Amazon forest greening. *PLoS One* **12**: e0180932.

Wang J, Krejci R, Giangrande S, *et al.* 2016. Amazon boundary layer aerosol concentration sustained by vertical transport during rainfall. *Nature* **539**: 416–9.

Wang J, Yang D, Detto M, *et al.* 2020. Multi-scale integration of satellite remote sensing improves characterization of dry-season green-up in an Amazon tropical evergreen forest. *Remote Sens Environ* **246**: 111865.

Wang X, Edwards RL, Auler AS, *et al.* 2017. Hydroclimate changes across the Amazon lowlands over the past 45,000 years. *Nature* **541**: 204–7.

Ward ND, Bianchi TS, Sawakuchi HO, *et al.* 2016. The reactivity of plant-derived organic matter and the potential importance of priming effects along the lower Amazon River. *J Geophys Res Biogeosciences* **121**: 1522–39.

Ward ND, Keil RG, Medeiros PM, *et al.* 2013. Degradation of terrestrially derived macromolecules in the Amazon River. *Nat Geosci* **6**: 530–3.

Werf GR van der, Randerson JT, Giglio L, *et al.* 2010. Global fire emissions and the contribution of deforestation, savanna, forest, agricultural, and peat fires (1997--2009). *Atmos Chem Phys* **10**: 11707–35.

West JJ, Fiore AM, Horowitz LW, and Mauzerall DL. 2006. Global health benefits of mitigating ozone pollution with methane emission controls. *Proc Natl Acad Sci* **103**: 3988–93.

Williams J, Keßel SU, Nölscher AC, *et al.* 2016. Opposite OH reactivity and ozone cycles in the Amazon rainforest and megacity Beijing: Subversion of biospheric oxidant control by anthropogenic emissions. *Atmos Environ* **125**: 112–8.

Williamson GB, Laurance WF, Oliveira AA, *et al.* 2000. Amazonian tree mortality during the 1997 El Nino drought. *Conserv Biol* **14**: 1538–42.

Wilson C, Gloor M, Gatti L V, *et al.* 2016. Contribution of regional sources to atmospheric methane over the Amazon Basin in 2010 and 2011. *Global Biogeochem Cycles* **30**: 400–20.

Wright JS, Fu R, Worden JR, *et al.* 2017. Rainforest-initiated wet season onset over the southern Amazon. *Proc Natl Acad Sci* **114**: 8481–6.

Wu J, Albert LP, Lopes AP, *et al.* 2016. Leaf development and demography explain photosynthetic seasonality in Amazon evergreen forests. *Science* **351**: 972–6.

Wu J, Serbin SP, Ely KS, *et al.* 2020. The response of stomatal conductance to seasonal drought in tropical forests. *Glob Chang Biol* **26**: 823–39.

Yáñez-Serrano AM, Bourtsoukidis E, Alves EG, *et al.* 2020. Amazonian biogenic volatile organic compounds under global change. *Glob Chang Biol* **26**: 4722–51.

Yáñez-Serrano AM, Nölscher AC, Bourtsoukidis E, *et al.* 2018. Monoterpene chemical speciation in a tropical rainforest: variation with season, height, and time of dayat the Amazon Tall Tower Observatory (ATTO). *Atmos Chem Phys* **18**: 3403–18.

Yáñez-Serrano AM, Nölscher AC, Williams J, *et al.* 2015. Diel and seasonal changes of biogenic volatile organic compounds within and above an Amazonian rainforest. *Atmos Chem Phys* **15**: 3359–78.

Young PJ, Archibald AT, Bowman KW, *et al.* 2013. Pre-industrial to end 21st century projections of tropospheric ozone from the Atmospheric Chemistry and Climate Model Intercomparison Project (ACCMIP). *Atmos Chem Phys* **13**: 2063–90.

Yu T and Zhuang Q. 2019. Quantifying global N2O emissions from natural ecosystem soils using trait-based biogeochemistry models. *Biogeosciences* **16**: 207–22.

Zeikus JG and Ward JC. 1974. Methane formation in living trees: a microbial origin. *Science* **184**: 1181–3.

Zemp DC, Schleussner C-F, Barbosa H, and Rammig A. 2017. Deforestation effects on Amazon forest resilience. *Geophys Res Lett* **44**: 6182–90.

Zeng N, Yoon J-H, Vintzileos A, *et al.* 2008. Dynamical prediction of terrestrial ecosystems and the global carbon cycle: A 25-year hindcast experiment. *Global Biogeochem Cycles* **22**.

SPA Technical-Scientific Secretariat New York
475 Riverside Drive, Suite 530
New York NY 10115
USA
+1 (212) 870-3920
spa@unsdsn.org

SPA Technical-Scientific Secretariat South America
Av. Ironman Victor Garrido, 623
São José dos Campos – São Paulo
Brazil
spasouthamerica@unsdsn.org